ACR No. L4D12

NATIONAL ADVISORY COMMITTEE FOR AERONAUTICS

WARTIME REPORT

ORIGINALLY ISSUED
April 1944 as
Advance Confidential Report L4D12

WIND-TUNNEL INVESTIGATION OF CONTROL-SURFACE CHARACTERISTICS

XVII - BEVELED-TRAILING-EDGE FLAPS OF 0.20, 0.30, AND 0.40 AIRFOIL CHORD ON AN NACA 0009 AIRFOIL

By Vernard E. Lockwood

Langley Memorial Aeronautical Laboratory
Langley Field, Va.

WASHINGTON

L - 666

NATIONAL ADVISORY COMMITTEE FOR AERONAUTICS

ADVANCE CONFIDENTIAL REPORT NO. L4D12

WIND-TUNNEL INVESTIGATION OF CONTROL-SURFACE CHARACTERISTICS

XVII - BEVELED-TRAILING-EDGE FLAPS OF 0.20, 0.30, AND 0.40 AIRFOIL CHORD ON AN NACA 0009 AIRFOIL

By Vernard E. Lockwood

SUMMARY

Force tests in two-dimensional flow have been made in the NACA 4- by 6-foot vertical tunnel to determine the aerodynamic characteristics of an NACA 0009 airfoil with flaps having chords 20, 30, and 40 percent of the airfoil chord and 20°, 30°, and 40° beveled trailing edges. The effect of a gap at the nose of the flap and of a rough leading edge was determined for the flaps equipped with the 30° beveled trailing edge.

The results indicated that, with a smooth leading edge, the increased trailing-edge angle on the flaps with sealed gaps decreased the slope of the control-fixed lift curve and the lift effectiveness. The increased trailing-edge angle generally reduced the hinge moment, that is, gave positive increments in the rate of change of hinge-moment coefficient with angle of attack and flap deflection. The hinge-moment characteristics also showed that, as the flap chord was increased, the bevel angle that gave the greatest reduction of hinge moments was increased.

Opening the gaps at the nose of the flaps caused a reduction in the slopes of the lift curves and a positive increment in the slopes of the hinge-moment curves. The addition of roughness strips to the nose of the airfoil produced similar results.

INTRODUCTION

Force tests of a number of NACA symmetrical airfoils have been made previous to the investigation reported herein for the purpose of providing data for the design of control surfaces. The modifications that have been previously tested include alterations of flap profile, flap nose shape, balance chord, gap size, and to some extent trailing-edge angle. Previous tests of airfoils have shown that considerable reduction in the hinge moments of flaps may be obtained by increasing the trailing-edge angle (references 1 to 4). The purpose of the present investigation is to show the effect of a wide range of trailing-edge angle on the aerodynamic characteristics of flaps of various chords. The investigation also includes tests of some of the models with an open gap at the nose of the flap and with a rough leading edge.

APPARATUS AND MODEL

The tests were made in the NACA 4- by 6-foot vertical tunnel described in reference 5 and modified as described in reference 6.

The 2-foot-chord by 4-foot-span model was made of laminated mahogany to the NACA 0009 profile ahead of each hinge axis. (See table I.) The model was tested with flaps having chords 20, 30, and 40 percent of the airfoil chord (0.20c, 0.30c, and 0.40c). Each flap had three interchangeable trailing-edge portions with included angles of 20°, 30°, and 40°. A plain nose with radius equal to approximately one-half the airfoil thickness at the hinge axis was used on each flap. The profiles of the flaps are defined in figure 1. An additional 0.30c flap, which had an asymmetric bevel with respect to the chord line and is hereinafter referred to as the 30° asymmetric flap, was tested. The 30° included angle at the trailing edge was divided to give a 10° bevel to one surface and a 20° bevel to the other surface and to make the bevel chords of the two surfaces equal. The gaps between the noses of the flaps and the cover plates were 0.002c. For most of the tests, the gap was sealed by sheet rubber glued to the nose of the flap and to the airfoil ahead of the flap.

For a few tests, the transition point on the airfoil was fixed by the addition of a strip 2 inches wide at the nose on each surface of the airfoil. The rough strip was composed of No. 60 carborundum fastened to the leading edge along the full span of the model.

TESTS

Some tests were made at a dynamic pressure of 15 pounds per square foot, which corresponds to a velocity of about 76 miles per hour at standard sea-level conditions. The effective Reynolds number for these tests was approximately 2,760,000. (Effective Reynolds number = Test Reynolds number × Turbulence factor. The turbulence factor for the NACA 4- by 6-foot vertical tunnel is 1.93.)

For the rest of the tests, the dynamic pressure was reduced to 11.25 pounds per square foot because insufficient power was available for continuous operation of the tunnel at a dynamic pressure of 15 pounds per square foot. The dynamic pressure of 11.25 pounds per square foot corresponds to a velocity of about 66 miles per hour and an effective Reynolds number of approximately 2,390,000.

The various model modifications and test Reynolds numbers are given in table II.

RESULTS

Symbols

Coefficients and symbols used herein are defined as follows:

c_l airfoil section lift coefficient (l/qc)

c_{d_o} airfoil section profile-drag coefficient (d_o/qc)

c_m airfoil section pitching-moment coefficient $\left(m/qc^2\right)$

c_{h_f} flap section hinge-moment coefficient $\left(h_f/qc_f^2\right)$

where

l airfoil section lift

d_o airfoil section profile drag

m airfoil section pitching moment about quarter-chord point of airfoil

h_f flap section hinge moment

c chord of basic airfoil with flap neutral

c_f flap chord

q dynamic pressure

and

α_o angle of attack for airfoil of infinite aspect ratio

δ_f flap deflection with respect to airfoil

ϕ flap trailing-edge angle; also referred to as bevel angle

$$c_{l_\alpha} = \left(\frac{\partial c_l}{\partial \alpha_o}\right)_{\delta_f}$$

$$c_{l_\delta} = \left(\frac{\partial c_l}{\partial \delta_f}\right)_{\alpha_o}$$

$$\alpha_\delta = \left(\frac{\partial \alpha_o}{\partial \delta_f}\right)_{c_l}$$

$$c_{h_\alpha} = \left(\frac{\partial c_{h_f}}{\partial \alpha_o}\right)_{\delta_f}$$

$$c_{h_\delta} = \left(\frac{\partial c_{h_f}}{\partial \delta_f}\right)_{\alpha_o}$$

$$\Delta c_{h_\delta} = c_{h_{\delta_p}} - c_{h_{\delta_b}}$$

$$\Delta c_{h_\alpha} = c_{h_{\alpha_p}} - c_{h_{\alpha_b}}$$

$$\Delta\phi = \phi_b - \phi_p$$

where

$$\phi_p = 11.6^\circ$$

Subscripts:

p airfoil-contour plain flap

b beveled flap for $\phi > 11.6^\circ$

The subscripts outside the parentheses represent the factors held constant during the measurement of the parameters.

Precision

The maximum error in angle of attack appears to be $\pm 0.2^\circ$. The small amount of lift obtained at an angle of attack of 0° for all tests with flap neutral indicates some inaccuracy in model construction or installation. Flap deflections were set within $\pm 0.2^\circ$. Tunnel corrections experimentally determined in the NACA 4- by 6-foot vertical tunnel were applied only to lift. The hinge moments are probably slightly higher than would be obtained in free air. The increments of profile-drag coefficient are believed to be accurate within ± 0.001 for small flap deflections and within ± 0.003 for large flap deflections and should be reasonably independent of tunnel effect although the absolute value is subject to an unknown correction.

Presentation of Data

The aerodynamic section characteristics of the NACA 0009 airfoil with the various flap arrangements tested are presented in figures 2 to 14. The lift, hinge-moment, and pitching-moment parameters are given in table II. The flap lift effectiveness α_δ is given as a function of flap chord ratio for the various trailing-edge angles in figure 15.

The data presented in figures 16 to 18 show flap section hinge-moment coefficient as a function of airfoil section lift coefficient resulting from the deflection of the 0.20c, 0.30c, and 0.40c flaps at $\alpha_0 = 0^\circ$. The effects of gap, trailing-edge angle, and leading-edge roughness are shown in parts (a), (b), and (c), respectively. The variation of flap section hinge-moment parameters with flap trailing-edge angle is given in figures 19 and 20 for the 0.20c, 0.30c, and 0.40c flaps with gaps sealed.

Increments of airfoil section profile-drag coefficient caused by flap deflection for the 0.20c, 0.30c, and 0.40c beveled flaps with various trailing-edge angles and gap conditions are shown in figures 21 to 23. Increments of profile-drag coefficient for the 0.30c plain flap of reference 6 are included in figure 22 for comparison.

The hinge-moment characteristics of the flaps with 0.002c and sealed gaps may be compared from figure 24 for an airfoil with a smooth leading edge. Similar data for airfoils with smooth and rough leading edges are given in figure 25 for flaps with sealed gaps to show the effect of fixing the transition point.

DISCUSSION

Airfoil with Smooth Leading Edge, Symmetric Flaps, and Sealed Gaps

Lift.- As is to be expected from references 1 and 2, the slope of the lift curve c_{l_α} (table II) was materially reduced by increasing the angle at the trailing edge ϕ from 20° to 30°; however, as ϕ was increased from 30° to 40°, this decrease was less marked. The variation of flap chord from 0.20c to 0.40c for constant trailing-edge angle ϕ decreased c_{l_α}. This decrease was probably due to the thickened flap profile.

The lift curves (figs. 2 to 4) show that, for positive angles of attack, the 0.20c beveled flaps gave greater lift and smaller hinge moments at flap deflections of 20° and 30° than the plain or airfoil-contour flap of reference 7. The 0.30c beveled flap (figs. 6 to 8) also gave greater lift and smaller hinge moments for a flap deflection of 30° than the plain flap of reference 6. The increased lift at these flap deflections is contrary to that shown by the airfoil of reference 2, for similar conditions.

The size of the trailing-edge angle had little effect on the angle of attack at which the airfoil stall occurred, but the increased flap chord decreased the angle of stall from 13° for the 0.20c flap to 11° for the 0.40c flap.

Figure 15 shows that, for a given flap chord, the flap lift-effectiveness parameter α_δ was decreased as the included angle at the trailing edge was increased and hence was less than for the corresponding plain flap. The value of α_δ, which is mainly a function of flap chord, increased with flap chord in about the same proportions for a constant angle ϕ as for a plain flap.

The control-free lift parameter $c_{l_{\alpha_{free}}}$ given in table II is valid only at $\alpha_o = \delta_f = 0^\circ$. Increasing the trailing-edge angle increased the slope of the control-free lift curve. The effect was qualitatively the same as that noted in reference 1.

Hinge moment.- An inspection of the hinge-moment-coefficient curves (figs. 2 to 14) indicates that linearity with angle of attack is restricted to the curves for the 20° beveled trailing edge at flap deflections of 0° to 5°. Other hinge-moment-coefficient curves are less linear than corresponding curves for the plain flaps.

The hinge-moment coefficients were generally smaller for the 0.20c and 0.30c beveled flaps than for the corresponding plain flaps for a given lift at $\alpha_o = 0^\circ$ (figs. 16 and 17). Likewise, the flaps with the 30° beveled trailing edge generally gave smaller hinge moments for a given lift than the flaps with the 20° beveled trailing edge.

The 20° and 30° bevels were effective in reducing hinge moments for the three flaps tested as is shown by the hinge-moment parameters plotted as a function of trailing-edge angle in figure 19. Replacing the 30° bevel by a 40° bevel changed the hinge-moment characteristics of the 0.20c flap only slightly in comparison with corresponding changes on the 0.30c and 0.40c flaps. On the 0.30c and 0.40c flaps, c_{h_α} and c_{h_δ} were made more positive by the 40° beveled flap. A comparison of the hinge-moment-coefficient curves indicates that, as the flap chord was increased, the bevel angle that gave the greatest reduction of hinge moments was increased.

The data from the present investigation do not appear to agree well with the results of the beveled-trailing-edge correlation of reference 4. The points in figure 20 representing the hinge-moment parameters from the present series of tests are considerably scattered from the results set forth in reference 4. Data on beveled controls obtained from various sources since the correlation was made show some disagreement and indicate that more factors should be taken into consideration than were given in the correlation in reference 4.

Pitching moment.- The values of $\left(\frac{\partial c_m}{\partial c_l}\right)_{\alpha_o}$ and $\left(\frac{\partial c_m}{\partial c_l}\right)_{\delta_f}$ (table II) give the position of the aerodynamic center of the airfoil with respect to the quarter-chord point. Increasing the trailing-edge angle shifted forward the center of the lift caused by angle of attack or by flap deflections. This shift was in the same direction as was noted for the NACA 0009 airfoil of reference 1 and the NACA 66(215)-014 airfoil of reference 2.

Drag.- Increments of airfoil section profile-drag coefficient Δc_{d_o} for the 0.20c, 0.30c, and 0.40c beveled flaps (figs. 21 to 23) were obtained by deducting the drag for the flap-neutral condition at an angle of attack of -6°, 0°, or 6° from the drag for the flap-deflected condition at the same angle of attack.

The 30° and 40° beveled flaps in general produced smaller increments of drag than the 20° beveled flap for angles of attack of 0° and 6°. The differences in drag for the various beveled flaps at $\alpha_o = \delta_f = 0°$ were within the experimental accuracy claimed for small flap deflections. The profile-drag coefficient for $\delta_f = 0°$ was approximately 0.0196, 0.0112, and 0.0188 for $\alpha_o = -6°$, 0°, and 6°, respectively.

Effect of Gap at Nose of Flap

An indication of the effect of a 0.002c gap at the nose of the flap on the aerodynamic characteristics of a flap with a beveled trailing edge may be seen from the parameter values of table II and figures 16(a) to 18(a). As expected from the results of reference 6, the lift parameters were numerically smaller and the hinge-moment parameters were more positive for flaps having 0.002c gaps than for flaps with sealed gaps.

The hinge-moment characteristics (fig. 24) of the 0.30c flap with a 30° beveled trailing edge and with open and sealed gap were typical of the various flaps tested with open gap.

The open gap usually gave larger increments of the airfoil section profile-drag coefficient for angles of attack of 6°, 0°, and -6° (figs. 21 to 23). The profile-drag coefficient at $\delta_f = 0°$ for the airfoil with smooth leading edge was approximately 0.0105 at $\alpha_o = 0°$ and 0.0170 at $\alpha_o = \pm 6°$.

Effect of a Rough Leading Edge

Fixing the transition point by means of a rough leading edge had some effect on the aerodynamic characteristics of the airfoil. The control-fixed lift parameters were numerically smaller and the hinge-moment parameters were more positive for the airfoil with rough leading edge than with smooth leading edge.

The rough leading edge gave a more gradual change in the slope of the lift curve near the stall and the maximum lift was less than for the smooth airfoil. The hinge-moment characteristics shown in figure 25 are typical for models with smooth and rough leading edges.

The addition of roughness strips to the leading edge gave an increase in the profile-drag coefficient of approximately 0.003 at $\alpha_o = \delta_f = 0°$.

Effect of Asymmetric Bevel

The aerodynamic section characteristics for the 30° asymmetric flap are given in figure 10. As was expected with the 20° bevel on the upper surface of the flap, the hinge-moment coefficients were negative at $\alpha_o = \delta_f = 0°$. The curve of hinge-moment coefficient as a function of angle of attack at $\delta_f = 0°$, like the curves for the 40° beveled flap, has a positive slope at negative angles of attack and, like the curves for the 20° beveled flap, has a negative slope at $\alpha_o > 3°$. A similar tendency is indicated in the variation of hinge-moment coefficient with flap deflection. Two curves, showing hinge-moment coefficient as a function of lift coefficient at $\alpha_o = 0°$, are given for the 30° asymmetric flap in figure 17(b), with each surface considered as the upper surface. The slopes of these curves are smaller than the corresponding slopes for the flaps with symmetric bevels.

CONCLUSIONS

Force tests in two-dimensional flow of flaps having chords 20, 30, and 40 percent of the airfoil chord and 20°, 30°, and 40° beveled trailing edges on an NACA 0009 airfoil have been made in the NACA 4- by 6-foot vertical tunnel. A comparison of the results of the tests of models having a smooth leading edge and a sealed flap with the results for plain flaps having chords 20 and 30 percent of the airfoil chord on an NACA 0009 airfoil indicated the following conclusions:

1. The increased trailing-edge angle and the increased thickness near the trailing edge reduced the slope of the control-fixed lift curve.

2. The flap lift effectiveness was reduced by the increase of the trailing-edge angle and hence was less than for the corresponding plain flaps.

3. An increase in the trailing-edge angle generally gave a more positive slope to the rate of change of hinge-moment coefficient with angle of attack and with flap deflection. The hinge-moment characteristics also showed that, as the flap chord was increased, the bevel angle that gave the greatest reduction of hinge moments was increased.

4. Aerodynamic centers of lift that result from varying the angle of attack and varying the flap deflection were generally shifted forward by an increase of the trailing-edge angle.

5. Opening the gaps at the nose of the flaps with a 30° beveled trailing edge decreased the slope of the control-fixed lift curve and decreased the flap effectiveness. The slopes of the curves of hinge-moment coefficient against angle of attack and flap deflection are more positive for the flap with open gap than with the sealed gap. The drag was generally higher for flaps with open than with sealed gaps.

6. Fixing the transition at the leading edge of the airfoil by the addition of roughness had an effect on the lift and hinge moment similar to that caused by opening the gap. The maximum lift was reduced by addition of the rough leading edge.

7. The asymmetric flap with 20° bevel on the upper surface and 10° bevel on the lower surface gave negative hinge moments at zero angle of attack and zero flap deflection. The hinge-moment-coefficient curve as a function of angle of attack at zero flap deflection had a positive slope at negative angles of attack and a negative slope at positive angles of attack greater than 3°.

Langley Memorial Aeronautical Laboratory,
National Advisory Committee for Aeronautics,
Langley Field, Va.

REFERENCES

1. Jones, Robert T., and Ames, Milton B., Jr.: Wind-Tunnel Investigation of Control-Surface Characteristics. V- The Use of a Beveled Trailing Edge to Reduce the Hinge Moment of a Control Surface. NACA ARR, March 1942.

2. Purser, Paul E., and Riebe, John M.: Wind-Tunnel Investigation of Control-Surface Characteristics. XV- Various Contour Modifications of a 0.30-Airfoil-Chord Plain Flap on an NACA 66(215)-014 Airfoil. NACA ACR No. 3L20, 1943.

3. Sears, Richard I.: Wind-Tunnel Data on the Aerodynamic Characteristics of Airplane Control Surfaces. NACA ACR No. 3L08, 1943.

4. Purser, Paul E., and Gillis, Clarence L.: Preliminary Correlation of the Effects of Beveled Trailing Edges on the Hinge-Moment Characteristics of Control Surfaces. NACA CB No. 3E14, 1943.

5. Wenzinger, Carl J., and Harris, Thomas A.: The Vertical Wind Tunnel of the National Advisory Committee for Aeronautics. NACA Rep. No. 387, 1931.

6. Sears, Richard I.: Wind-Tunnel Investigation of Control-Surface Characteristics. I- Effect of Gap on the Aerodynamic Characteristics of an NACA 0009 Airfoil with a 30-Percent-Chord Plain Flap. NACA ARR, June 1941.

7. Sears, Richard I., and Purser, Paul E.: Wind-Tunnel Investigation of Control-Surface Characteristics. XIV- NACA 0009 Airfoil with a 20-Percent-Chord Double Plain Flap. NACA ARR No. 3F29, 1943.

TABLE I.- ORDINATES FOR NACA 0009 AIRFOIL

[Station and ordinates in percent of airfoil chord]

Station	Ordinate
0	0
1.25	1.42
2.5	1.96
5	2.67
7.5	3.15
10	3.51
15	4.01
20	4.30
25	4.46
30	4.50
40	4.35
50	3.97
60	3.42
70	2.75
80	1.97
90	1.09
95	.60
100	(.10)
100	0
L.E. radius: 0.89	

TABLE II.- PARAMETERS FOR NACA 0009 AIRFOIL WITH BEVELED-TRAILING-EDGE FLAPS

[Parameters measured over small range of angle of attack and flap deflection where curves are nearly linear. Because of general nonlinearity of curves, parameters should be used only with figs. 2 to 14. Measurements of c_{h_α} limited to range of α from -3° to 3°; c_{h_δ} to range of δ_f from -5° to 5°.]

Description of model			Figure	Test Reynolds number	Parameters						
Trailing-edge angle, ϕ (deg)	Condition of airfoil L.E.	Gap at flap nose			$\left(\frac{\partial c_l}{\partial \alpha_o}\right)_{\delta_f}$	$\left(\frac{\partial \alpha_o}{\partial \delta_f}\right)_{c_l}$	$\left(\frac{\partial c_l}{\partial \alpha_o}\right)_{free}$	$\left(\frac{\partial c_{h_f}}{\partial \alpha_o}\right)_{\delta_f}$	$\left(\frac{\partial c_{h_f}}{\partial \delta_f}\right)_{\alpha_o}$	$\left(\frac{\partial c_m}{\partial c_l}\right)_{\delta_f}$	$\left(\frac{\partial c_m}{\partial c_l}\right)_{\alpha_o}$
				0.20c flap							
[a]11.6	Smooth	Sealed	------	--------	0.098	-0.44	---------	-0.0050	-0.0115	-------	-------
20	--do--	--do--	2	2.76×10^6	.098	-.42	0.095	-.0006	-.0079	0.022	-0.190
30	--do--	--do--	3	2.76	.094	-.41	.121	.0035	-.0044	.032	-.184
40	--do--	--do--	4	2.76	.095	-.40	.122	.0030	-.0042	.032	-.180
30	Rough	--do--	3	2.76	.090	-.40	.141	.0051	-.0035	.023	-.179
30	Smooth	0.002c	5	2.76	.092	-.36	.163	.0047	-.0022	.036	-.180
				0.30c flap							
[a]11.6	Smooth	Sealed	------	--------	0.098	-0.57	---------	-0.0075	-0.0130	-------	------
20	--do--	--do--	6	2.39×10^6	.095	-.56	0.076	-.0034	-.0101	0.022	-0.150
30	--do--	--do--	7	2.76	.090	-.53	.101	.0010	-.0044	.042	-.142
40	--do--	--do--	8	2.39	.089	-.52	.176	.0048	-.0026	.048	-.141
30	Rough	--do--	7	2.76	.089	-.51	.122	.0025	-.0034	.045	-.143
30	--do--	0.002c	9	2.76	.088	-.50	.088	.0000	-.0017	.049	-.130
30	Smooth	--do--	9	2.76	.089	-.50	.144	.0036	-.0029	.049	-.140
[b]30	--do--	Sealed	10	2.39	.093	-.54	.122	.0016	-.0028	.042	-.143
				0.40c flap							
[a]11.6	Smooth	Sealed	------	--------	0.098	-0.68	---------	-0.0101	-0.0145	-------	------
20	--do--	--do--	11	2.39×10^6	.094	-.68	0.066	-.0048	-.0109	0.033	-0.113
30	--do--	--do--	12	2.76	.088	-.64	.095	.0006	-.0049	.050	-.096
40	--do--	--do--	13	2.39	.086	-.62	.128	.0035	-.0026	.063	-.095
30	Rough	--do--	12	2.76	.084	-.62	.116	.0022	-.0036	.057	-.090
30	Smooth	0.002c	14	2.76	.085	-.56	.121	.0019	-.0025	.049	-.107

[a]For airfoil-contour plain flap from reference

[b]Asymmetric flap.

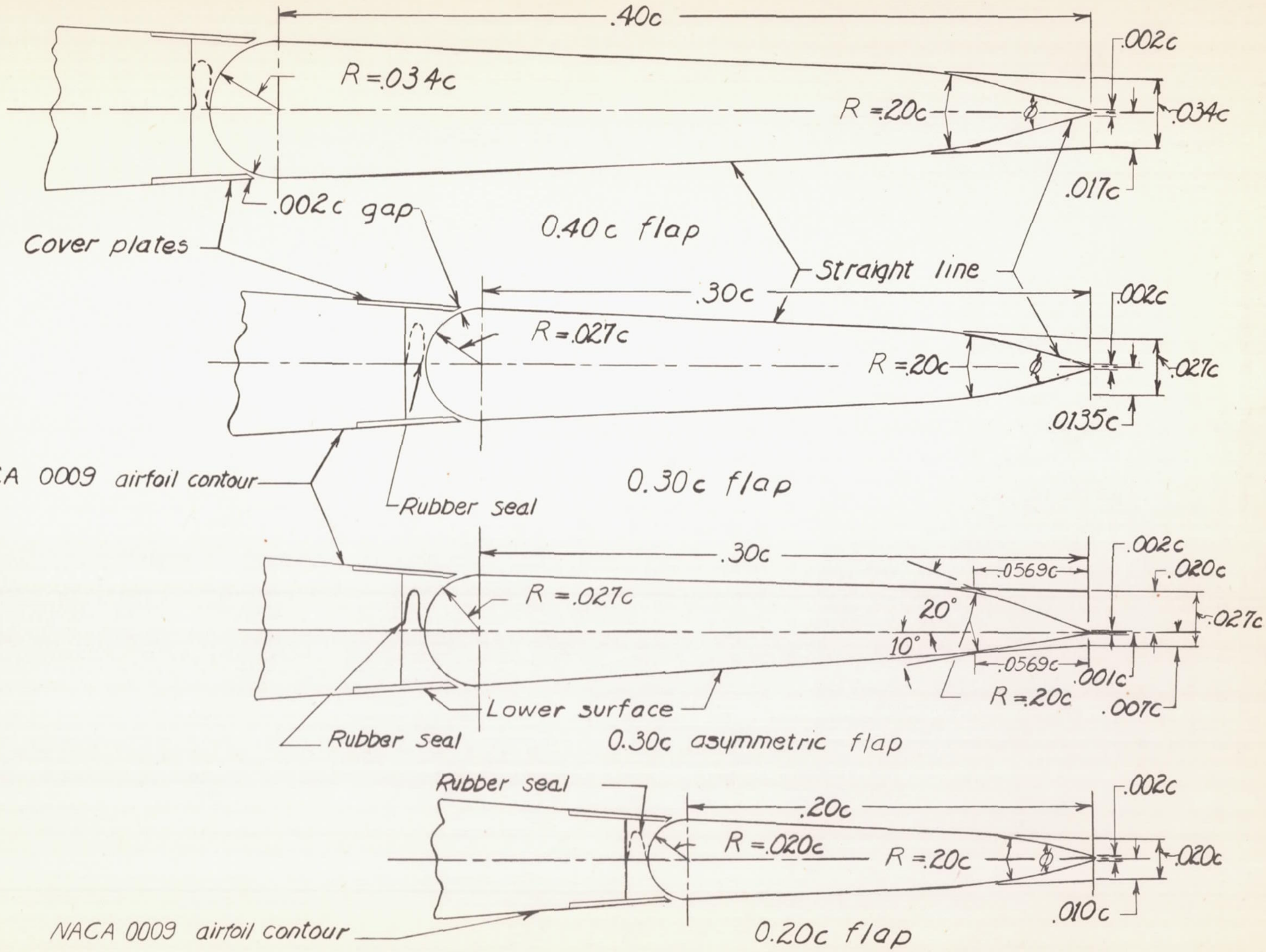

Figure 1. -Details of bevel-trailing-edge flaps tested on NACA 0009 air-foil.

L-666

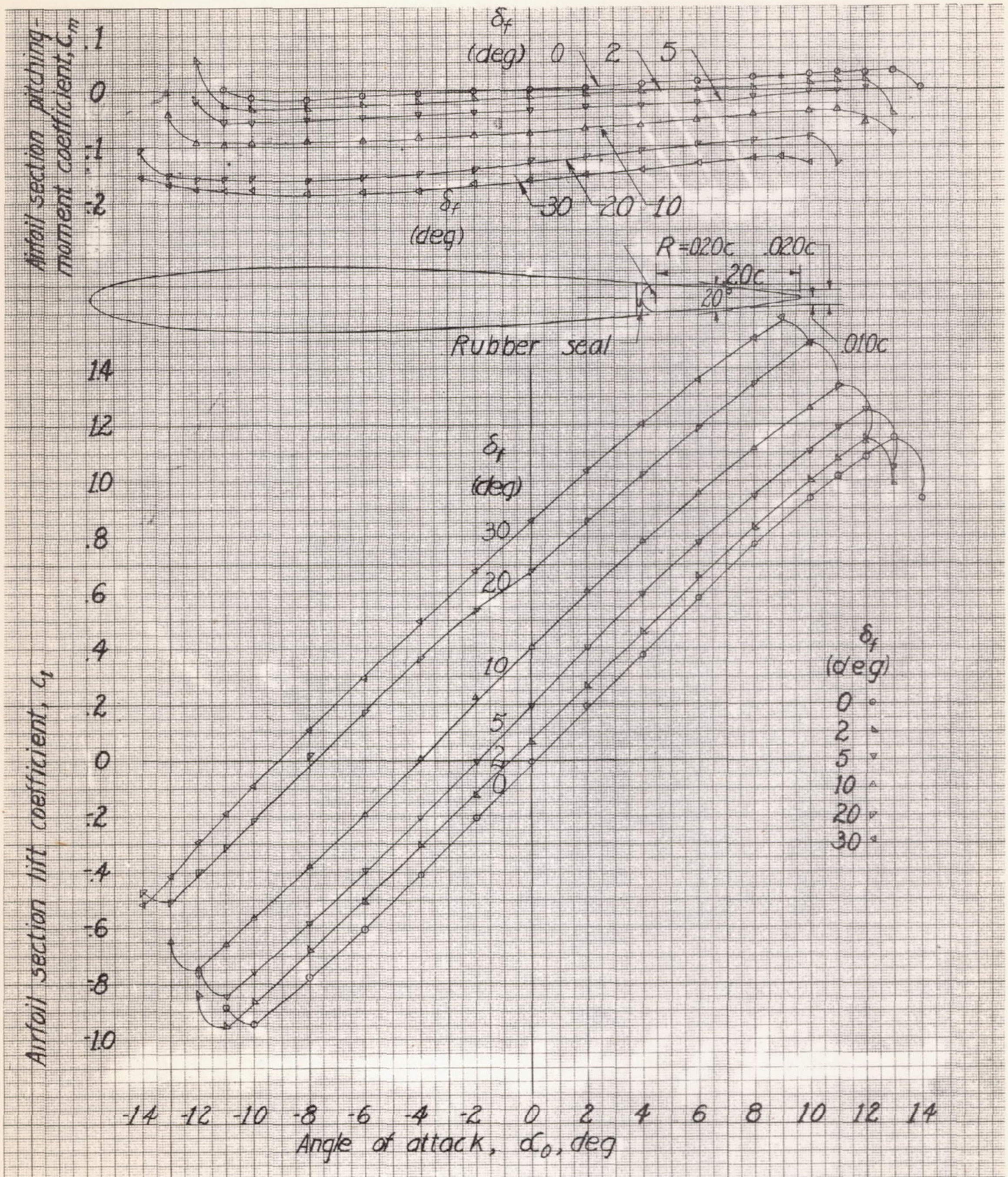

Figure 2.-Aerodynamic section characteristics of NACA 0009 airfoil having 0.20c flap with 20° beveled trailing edge. Sealed gap; q = 15 pounds per square foot.

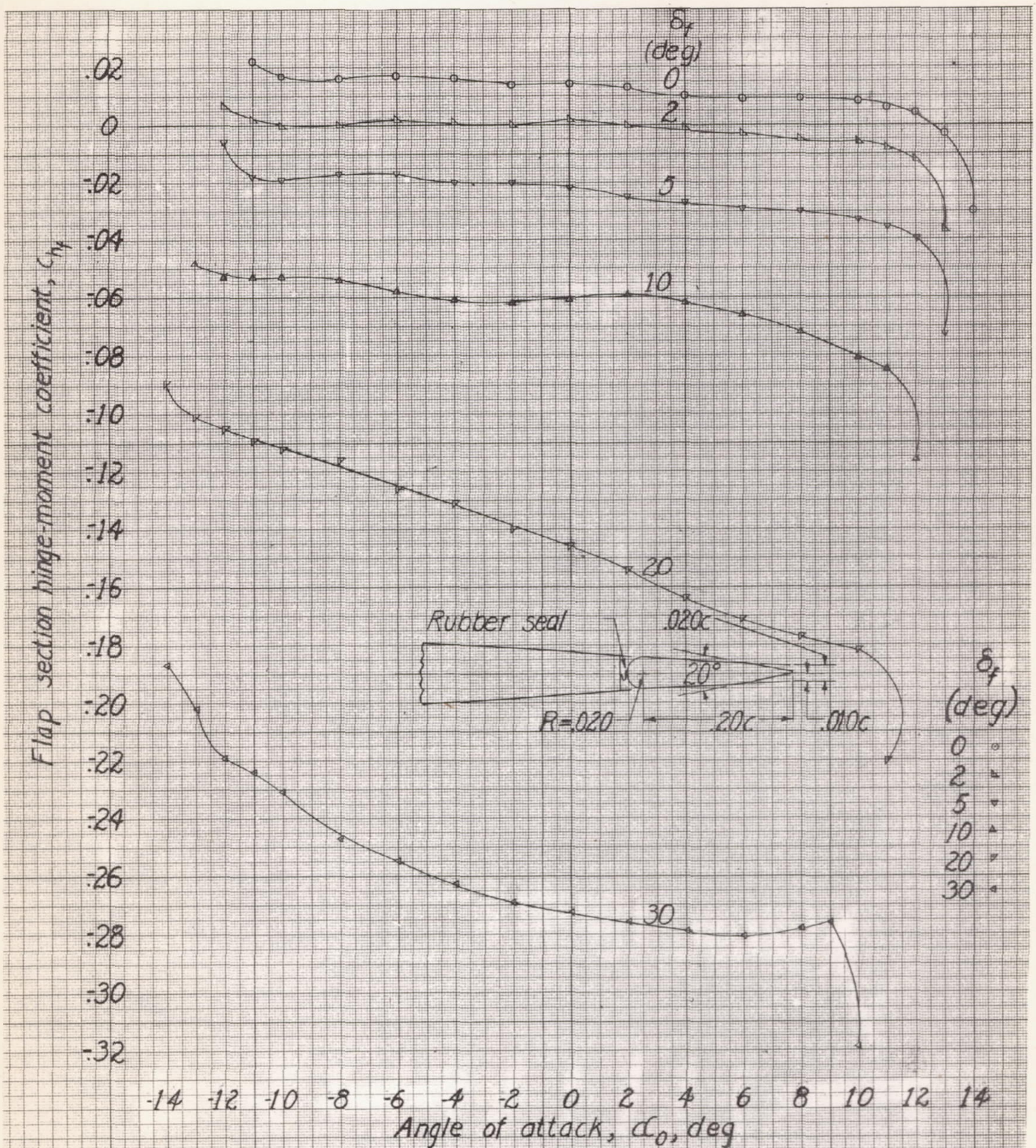

Figure 2.- Concluded.

L-666

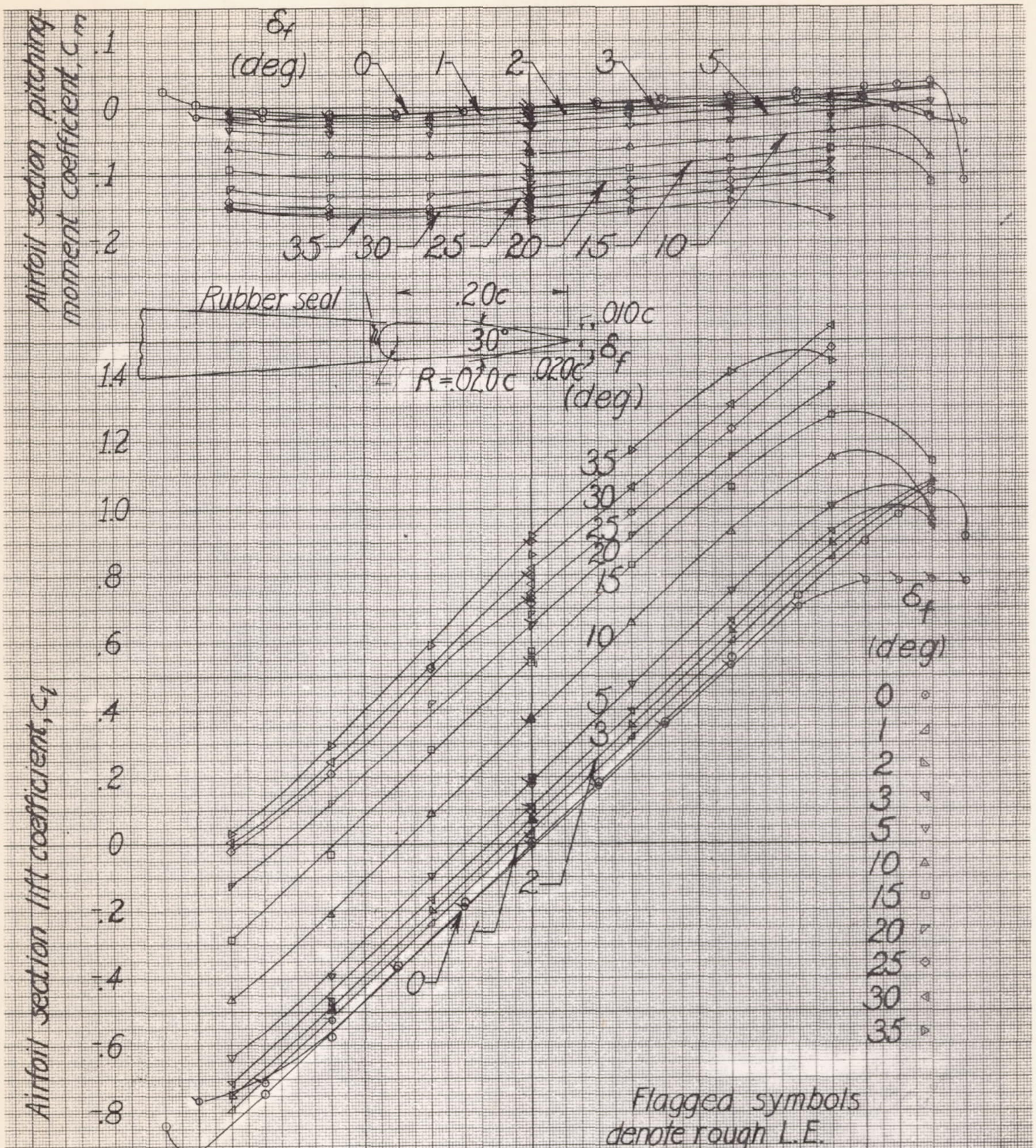

Figure 3.- Aerodynamic section characteristics of an NACA 0009 airfoil having 0.20c flap with 30° beveled trailing edge. Sealed gap; q = 15 pounds per square foot.

L-666

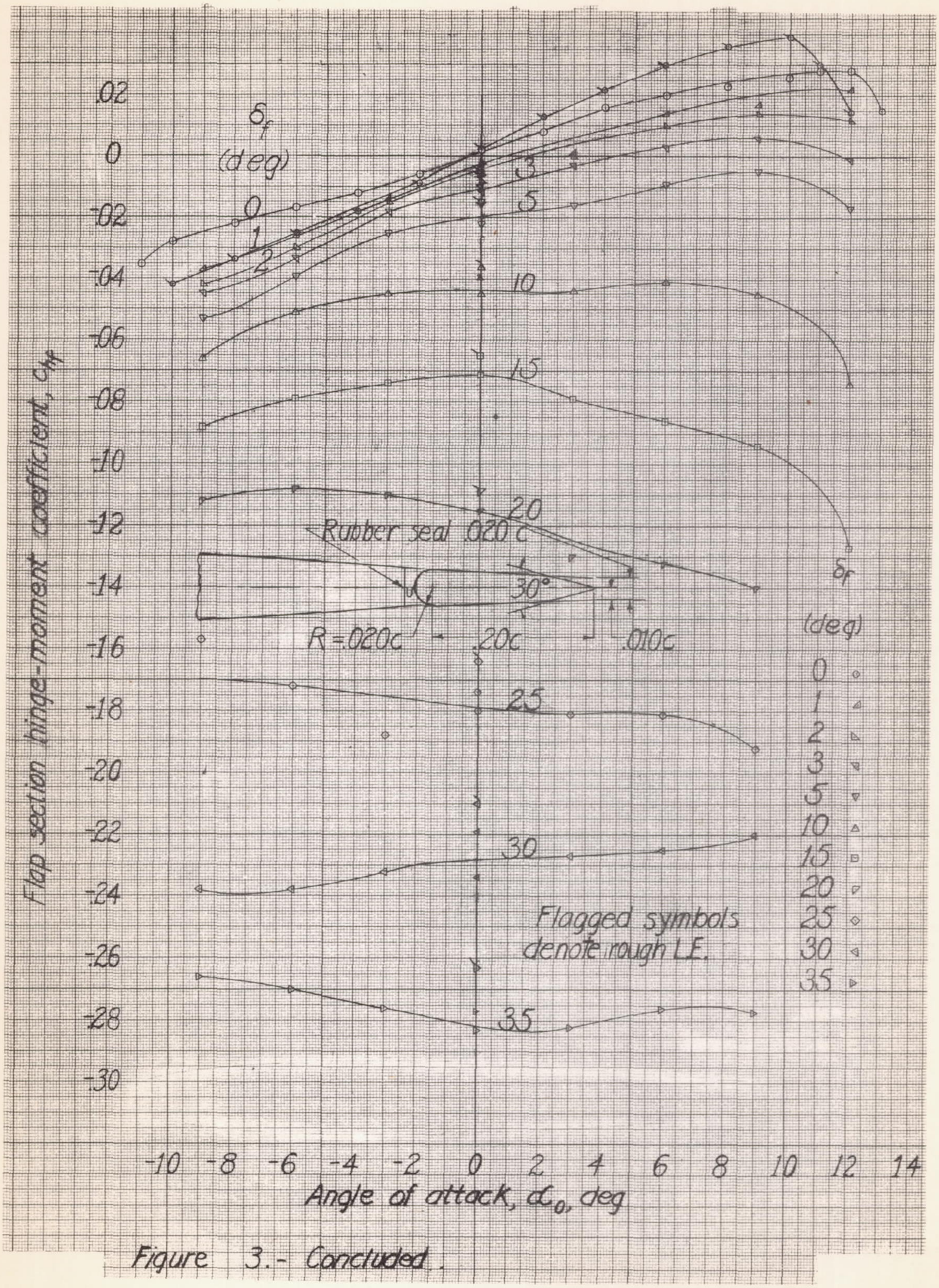

Figure 3.- Concluded.

L-666

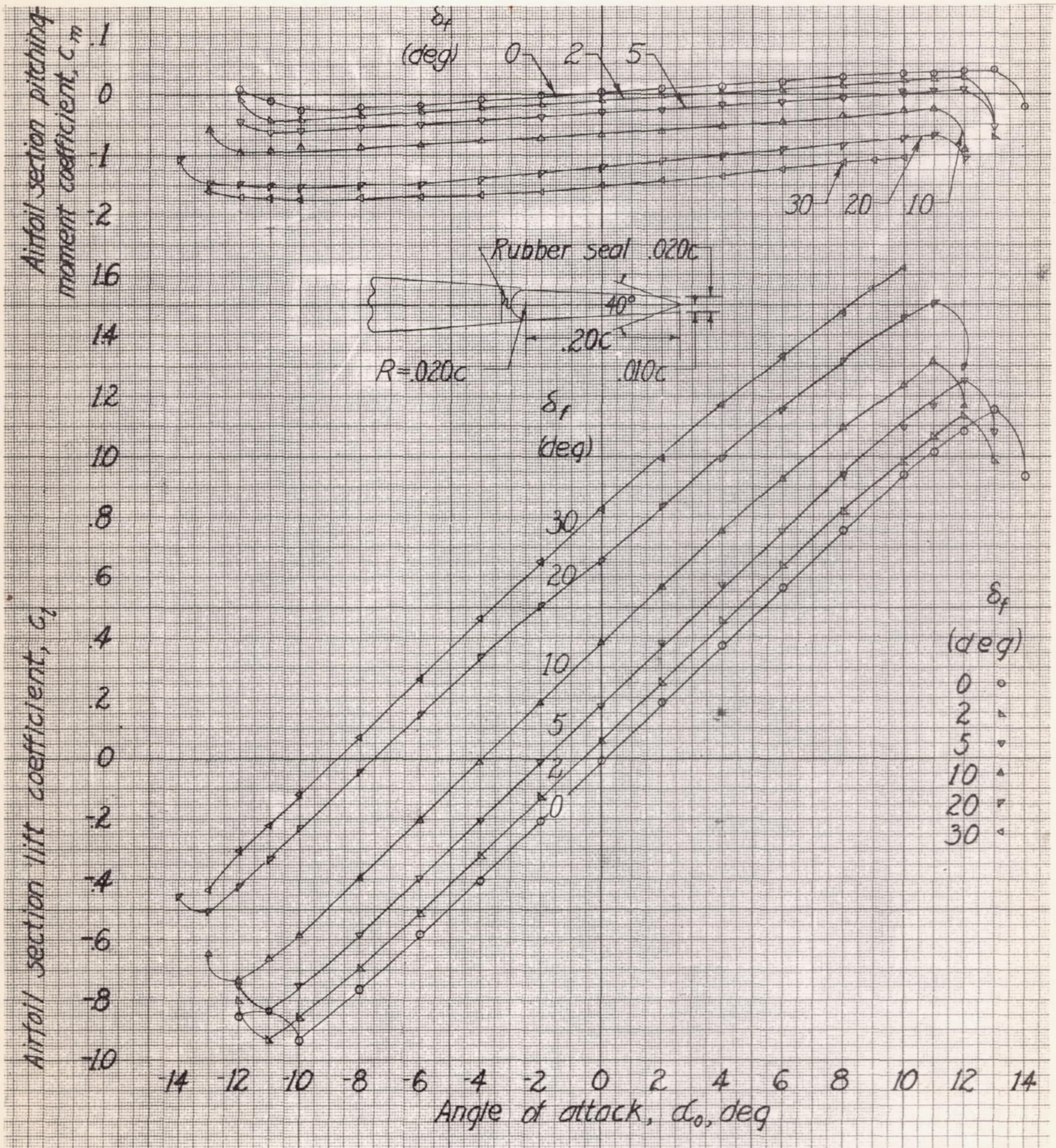

Figure 4.- Aerodynamic section characteristics of an NACA 0009 airfoil having 0.20c flap with 40° beveled trailing edge. Sealed gap; q=15 pounds per square foot.

L-666

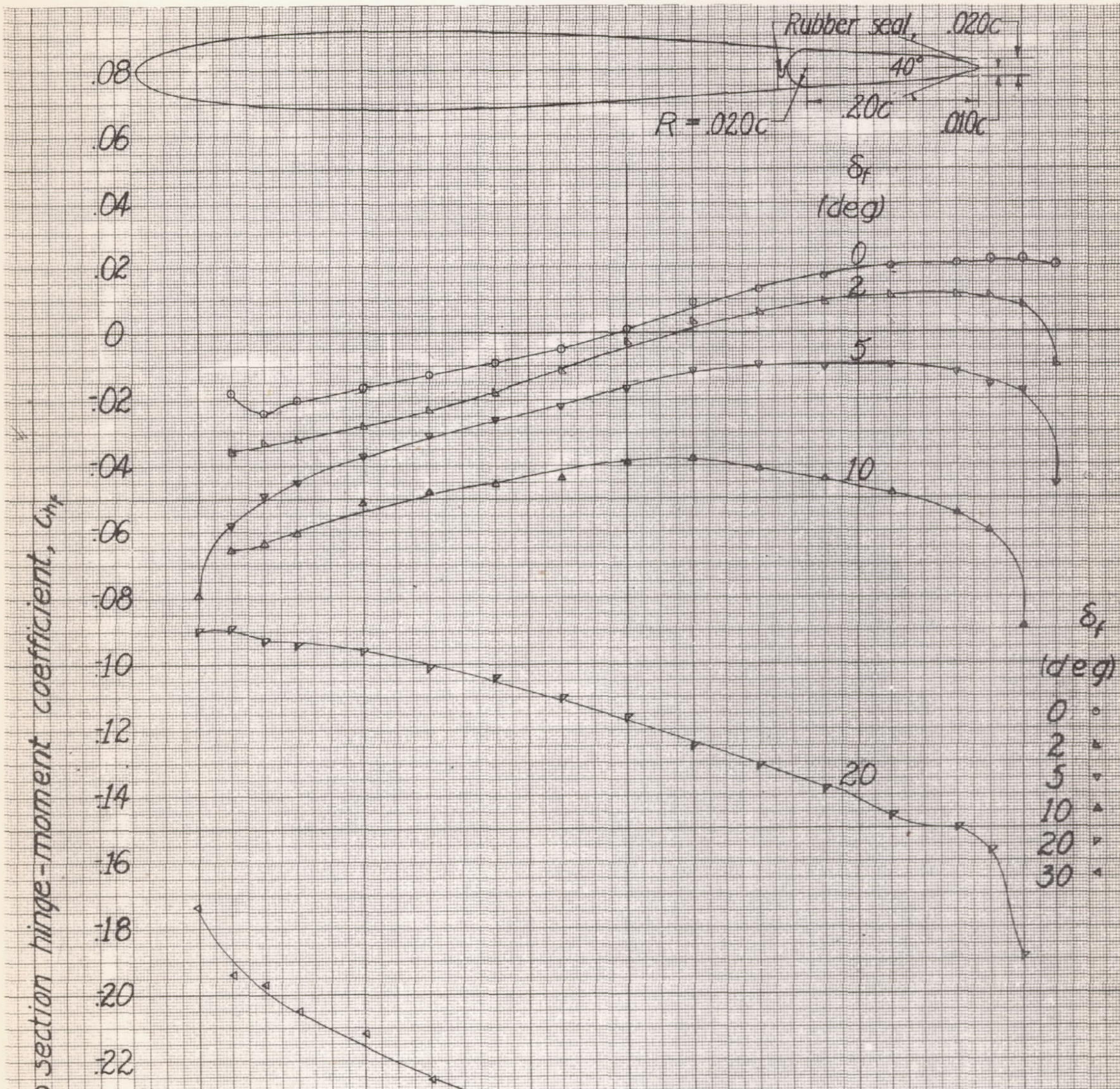

Figure 4.- Concluded.

L-666

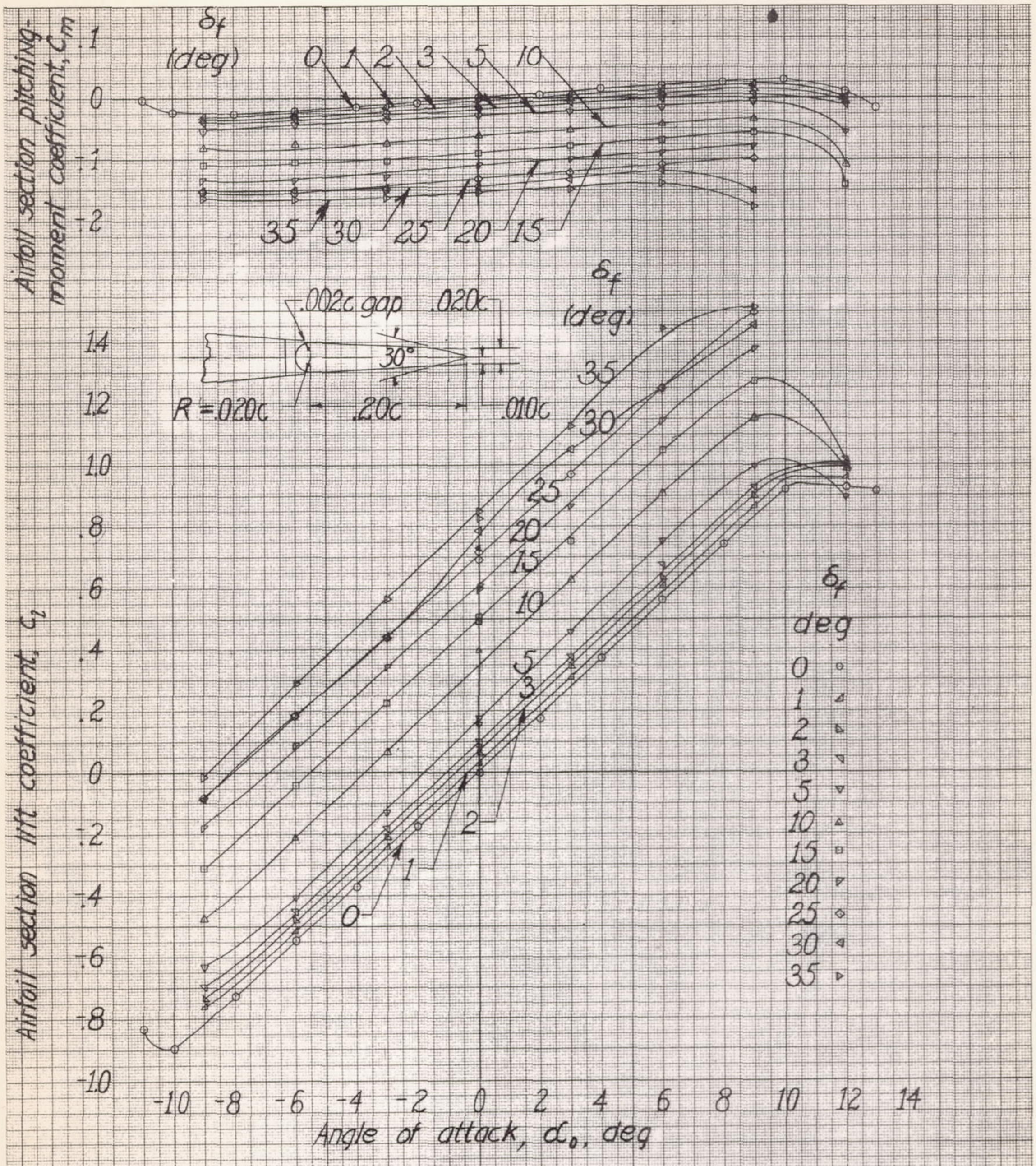

Figure 5.- Aerodynamic section characteristics of an NACA 0009 airfoil having 0.20c flap with 30° beveled trailing edge. 0.002c gap; q=15 pounds per square foot.

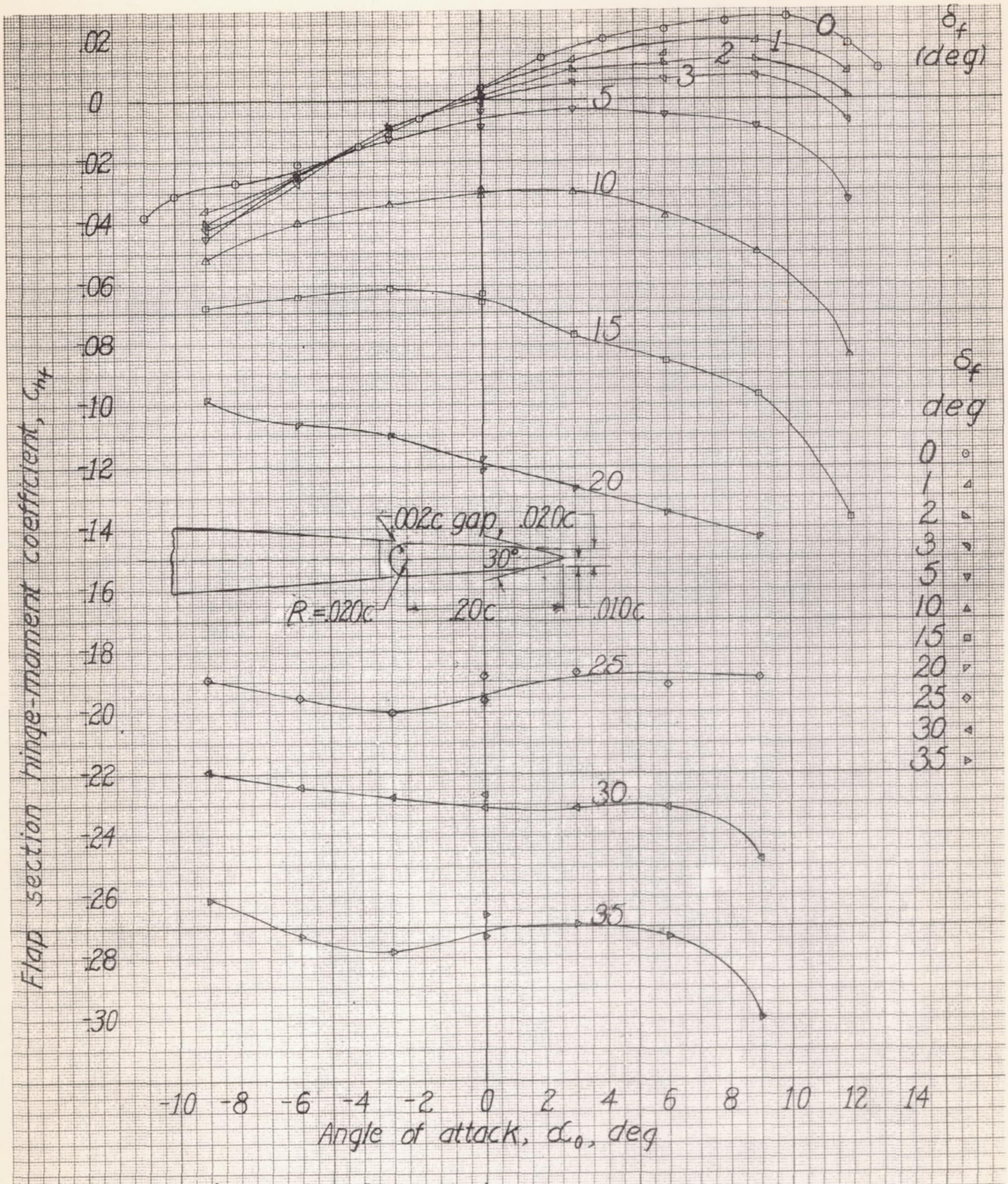

Figure 5.- Concluded.

L-666

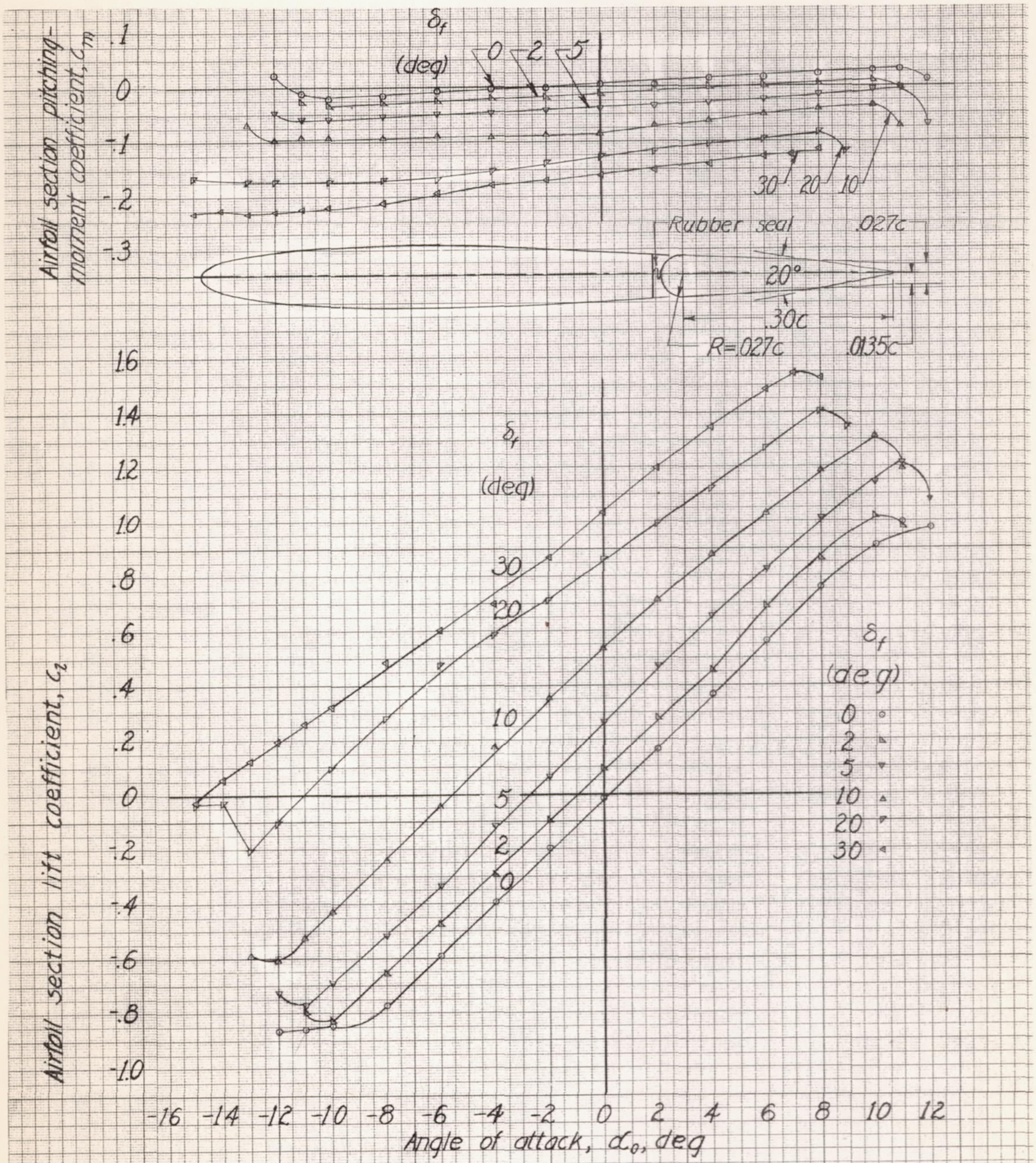

Figure 6.-Aerodynamic section characteristics of an NACA 0009 airfoil having 0.30c flap with 20° beveled trailing edge. Sealed gap; q=11.25 pounds per square foot.

L-666

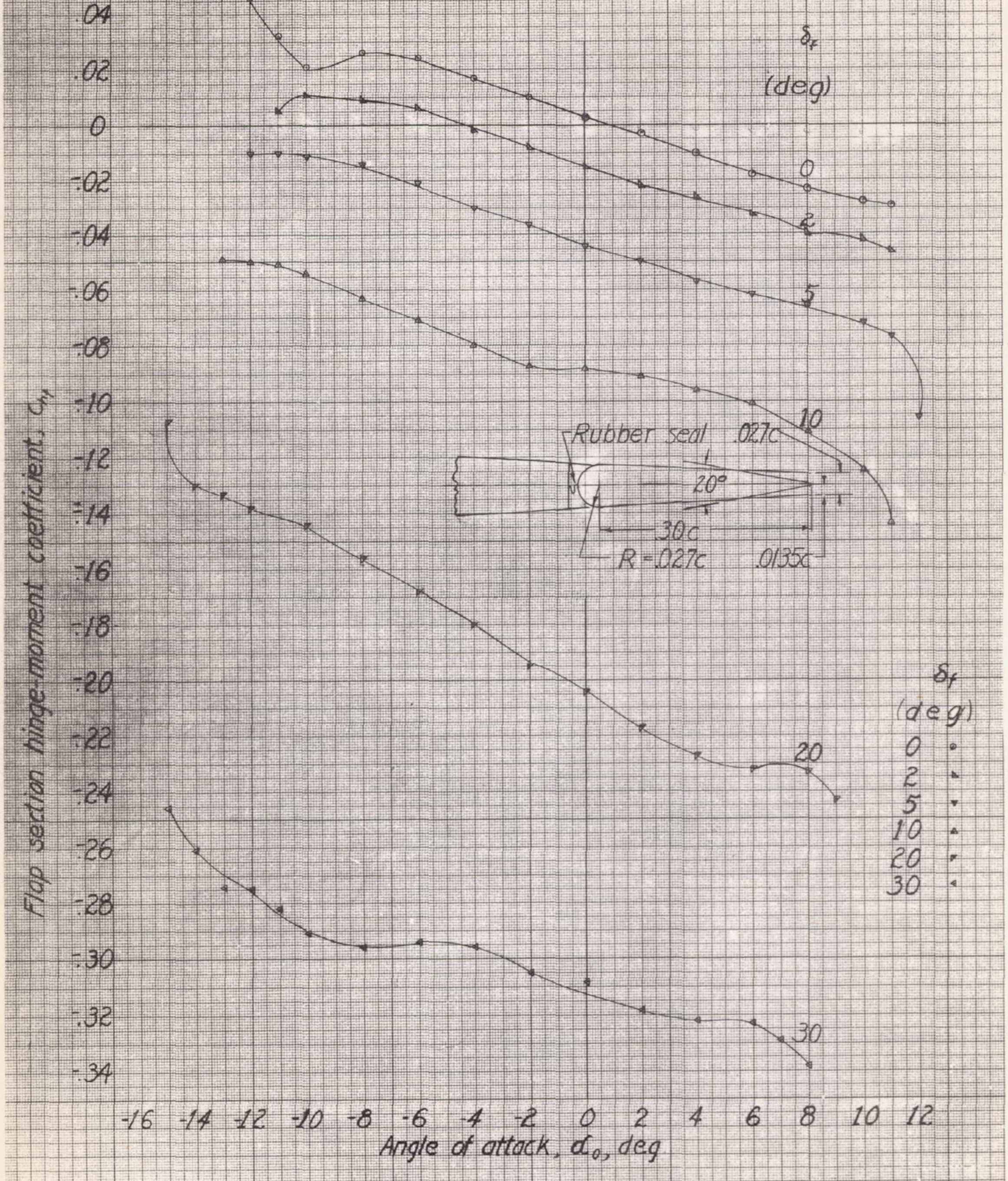

Figure 6. - Concluded.

L-666

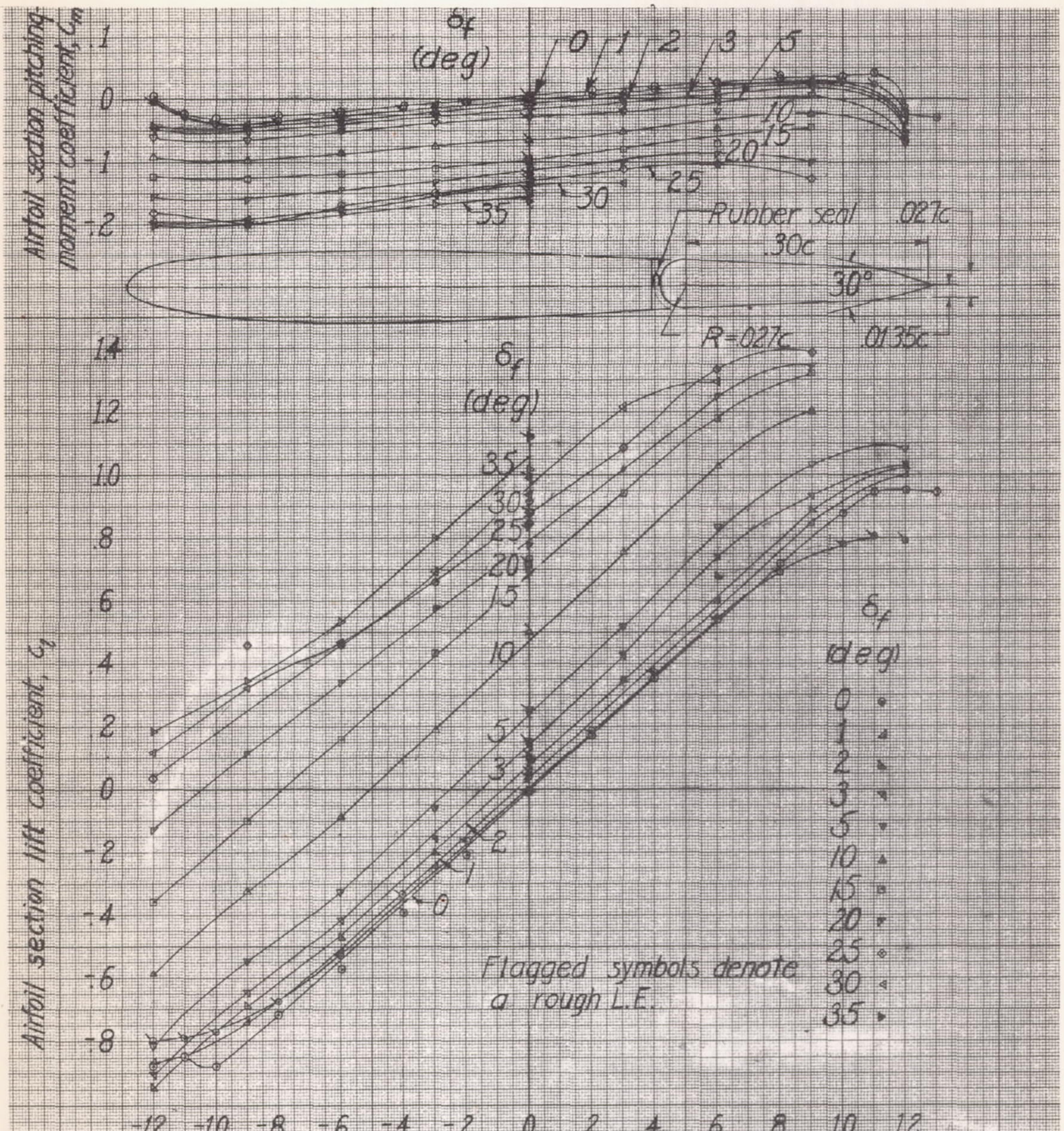

Figure 7.-Aerodynamic section characteristics of an NACA 0009 airfoil having 0.30c flap with 30° beveled trailing edge. Sealed gap; q=15 pounds per square foot.

L-666

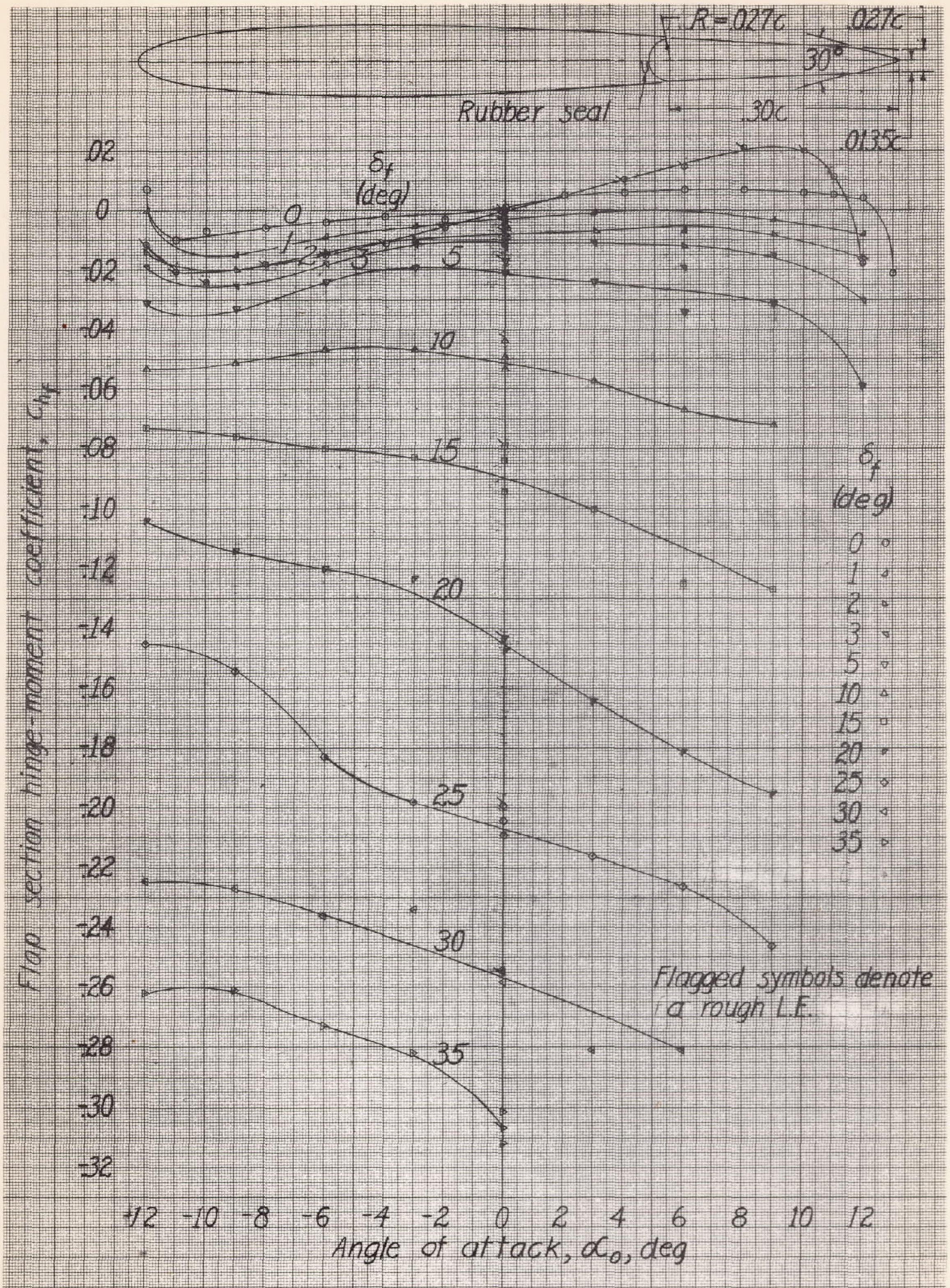

Figure 7- Concluded.

L-666

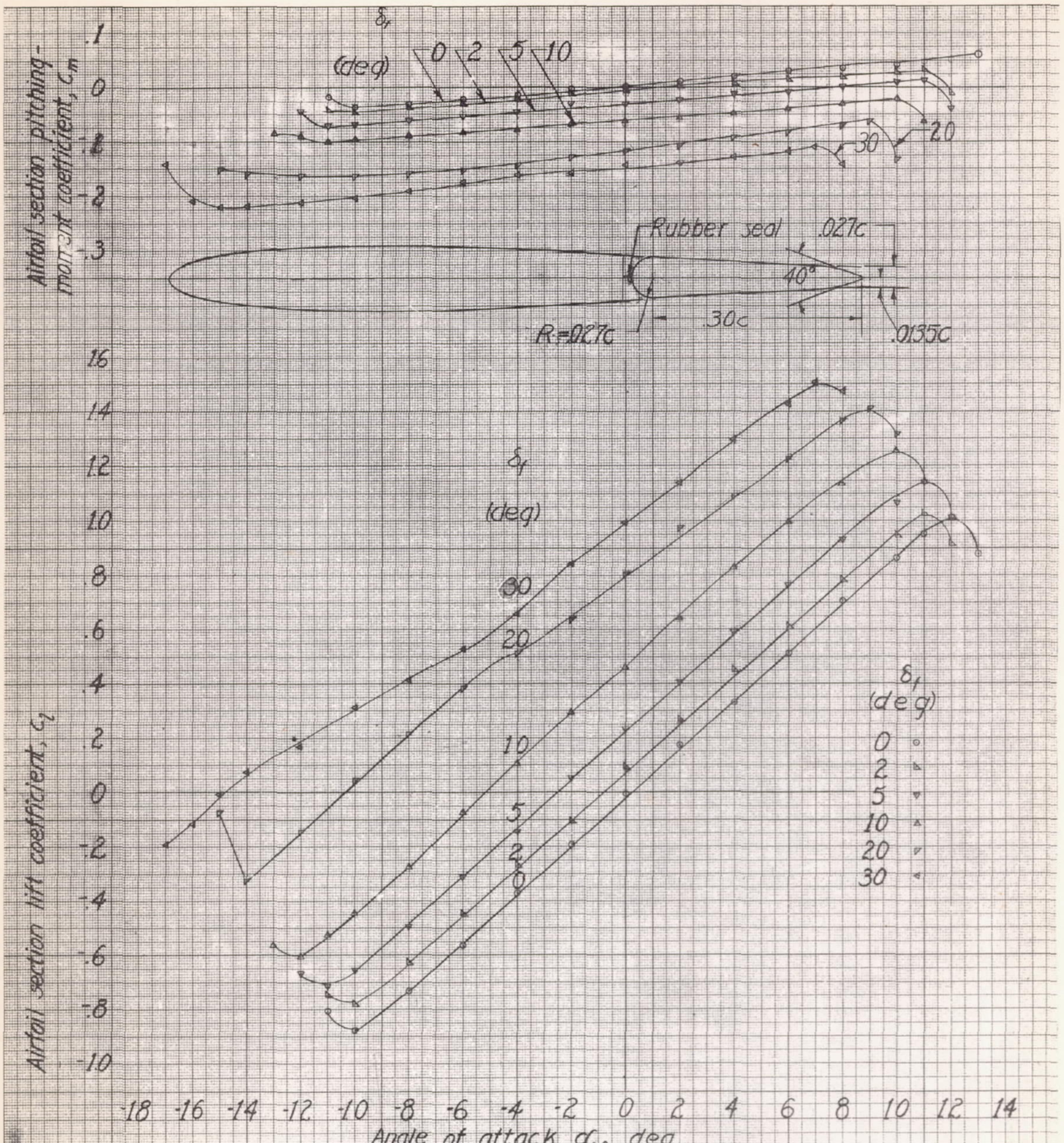

Figure 8.- Aerodynamic section characteristics of NACA 0009 airfoil having 0.30c flap with 40° beveled trailing edge. Sealed gap; q=11.25 pounds per square foot.

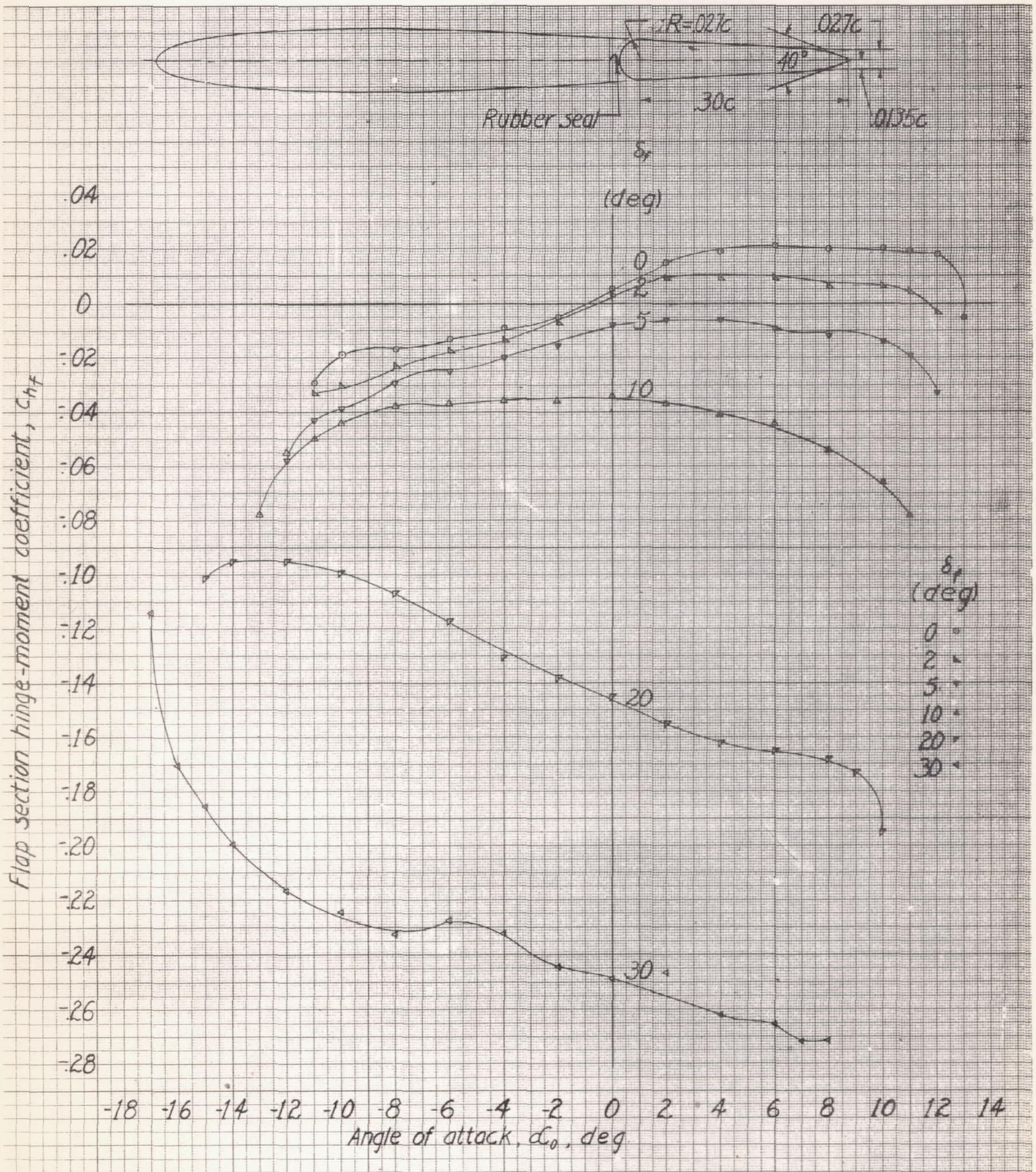

Figure 8. - Concluded.

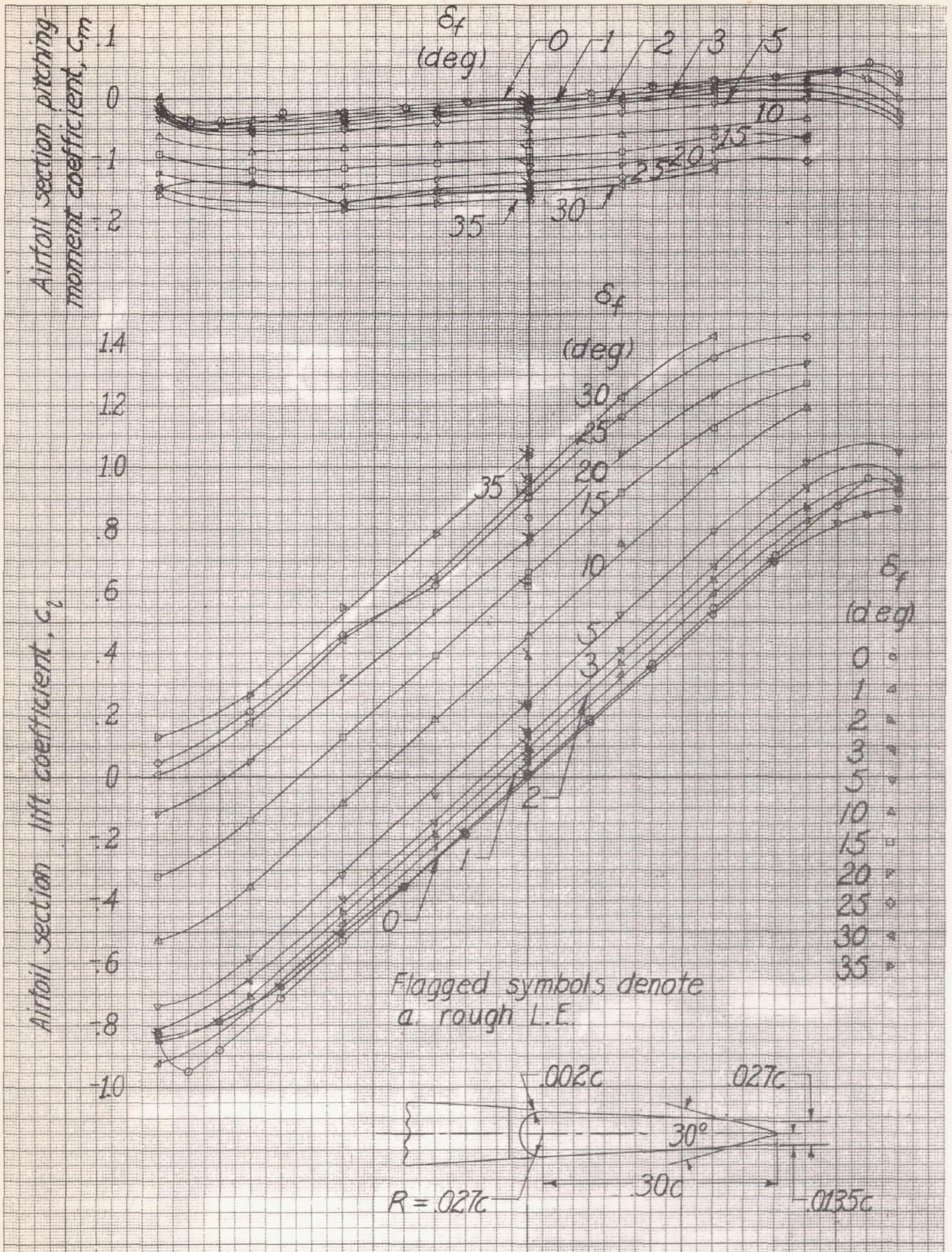

Figure 9.- Aerodynamic section characteristics of an NACA 0009 airfoil having 0.30c flap with 30° beveled trailing edge. 0.002c gap; q = 15 pounds per square foot.

L-666

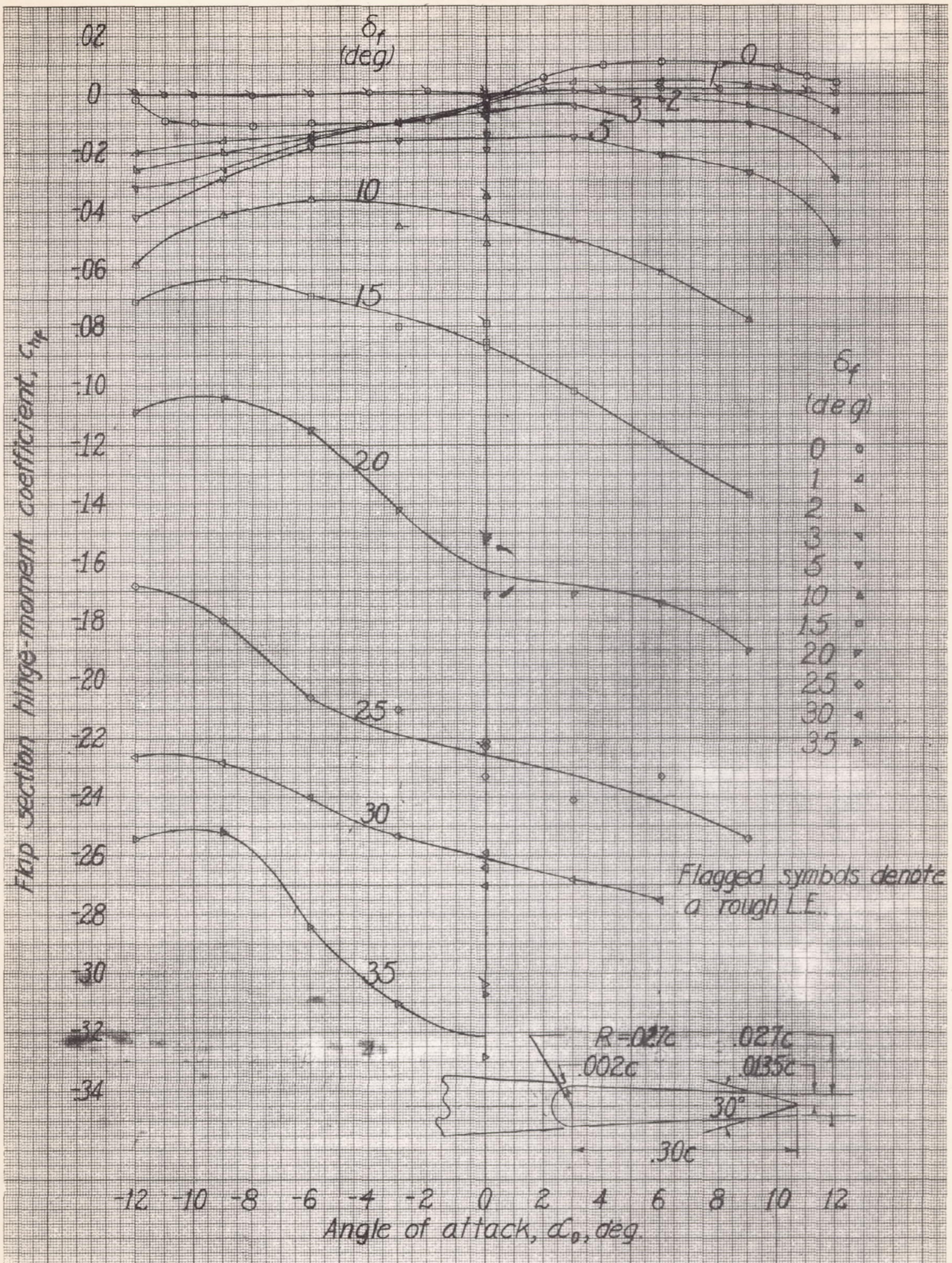

Figure 9.- Concluded.

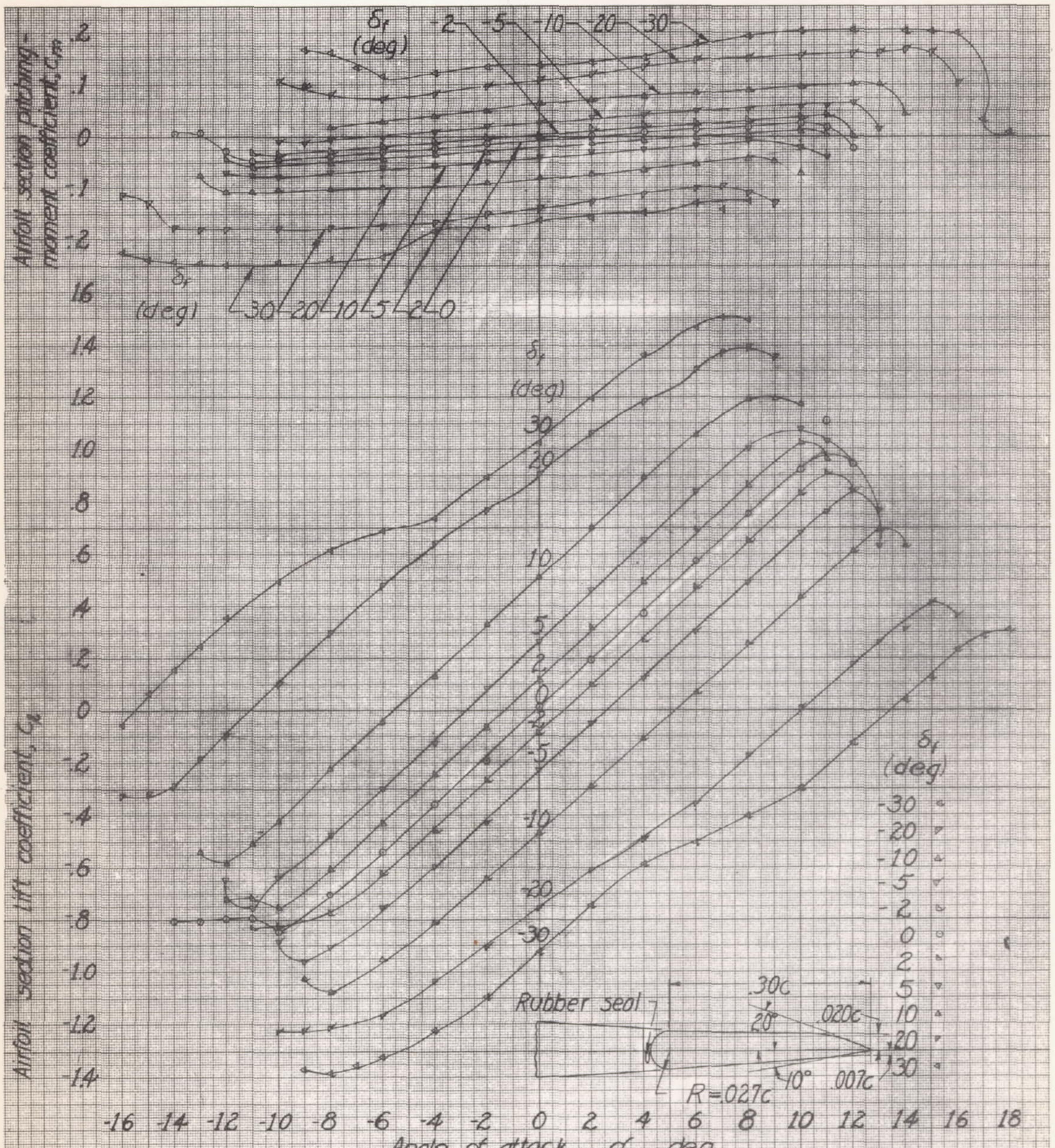

Figure 10.- Aerodynamic section characteristics of an NACA 0009 airfoil having 0.30c flap with asymmetric beveled trailing edge. Sealed gap; q = 11.25 pounds per square foot.

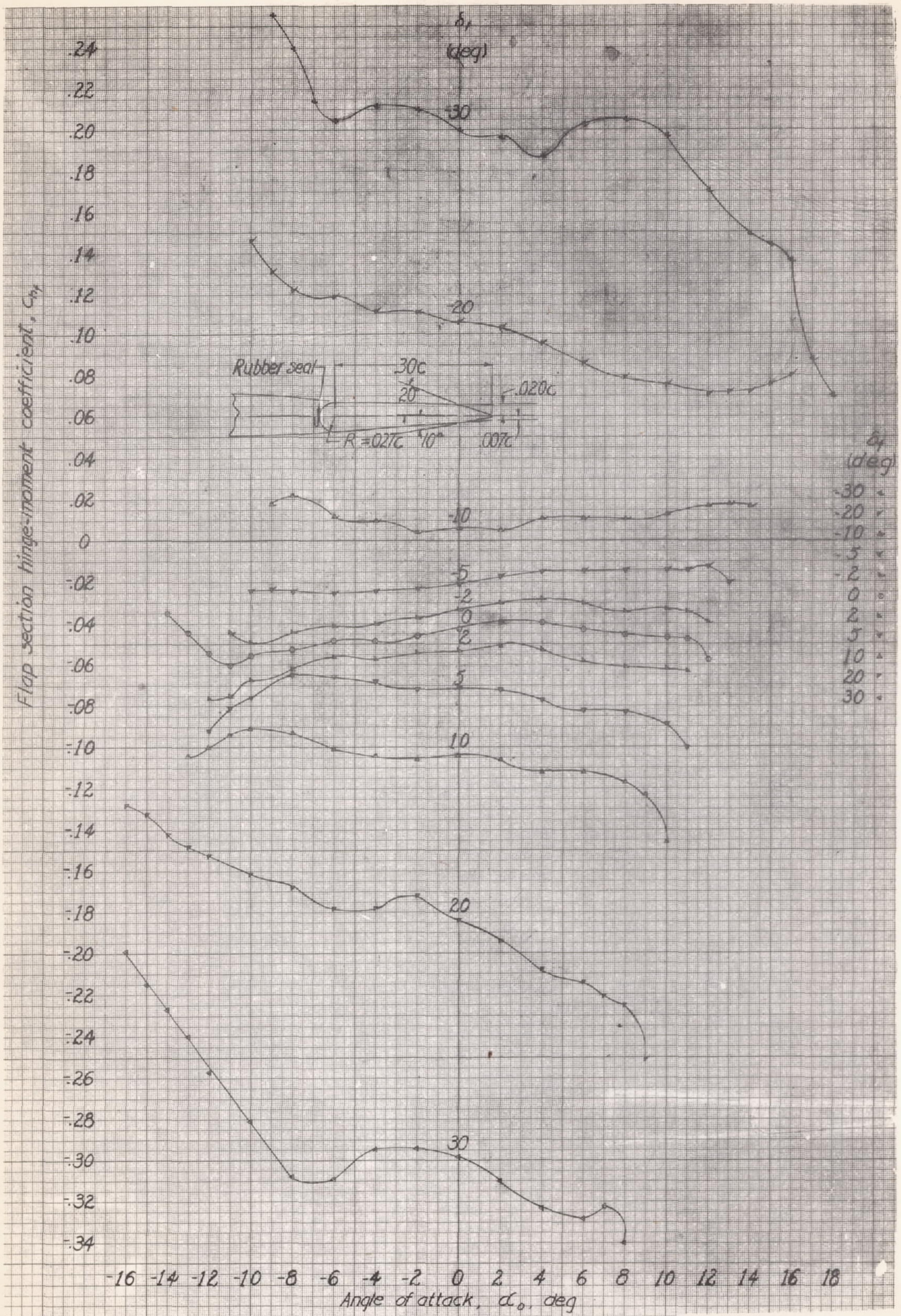

Figure 10- Concluded.

L-666

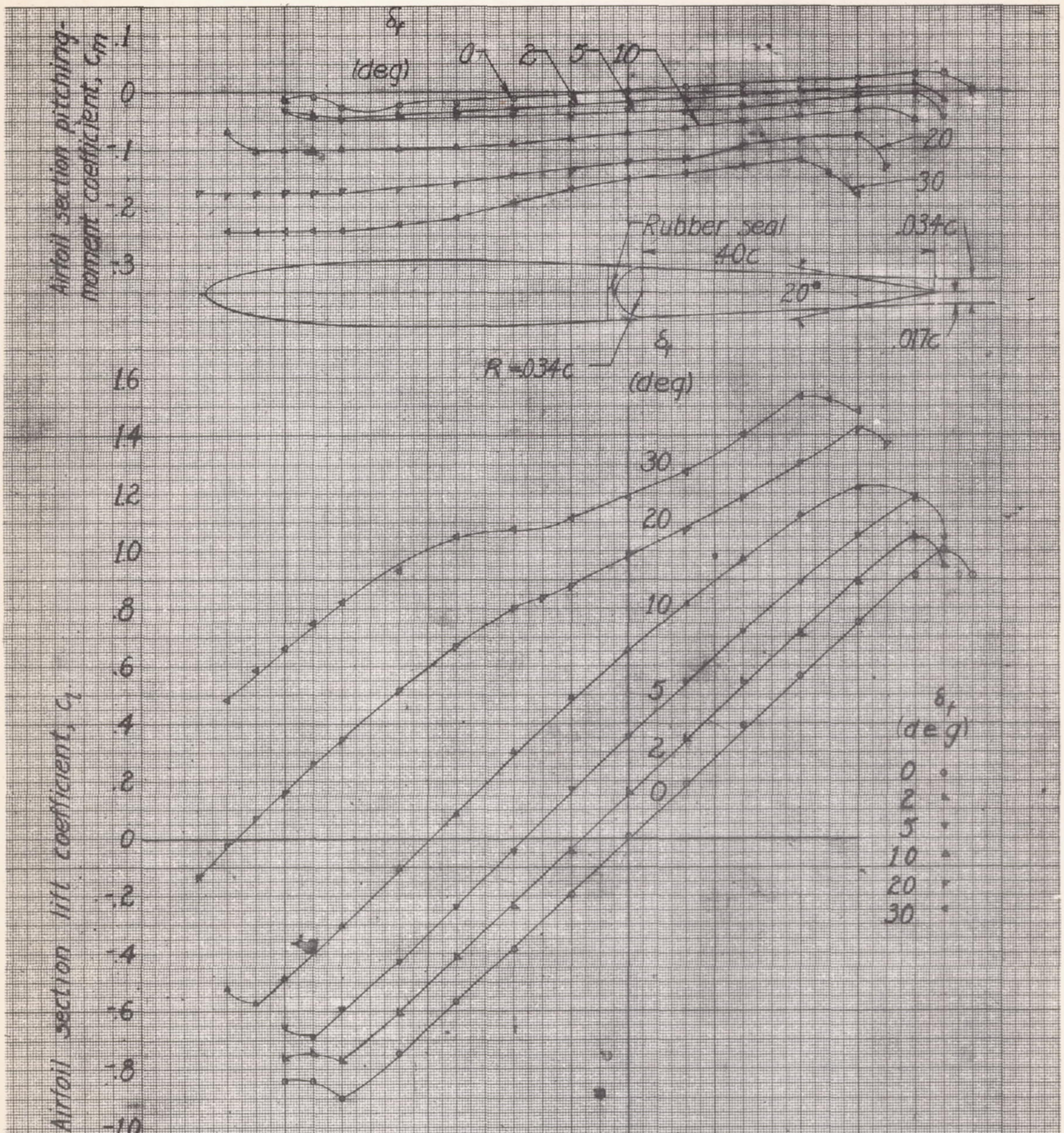

Figure 11.- Aerodynamic section characteristics of an NACA 0009 airfoil having 0.40c flap with 20° beveled trailing edge. Sealed gap; q=11.25 pounds per square foot.

L-666

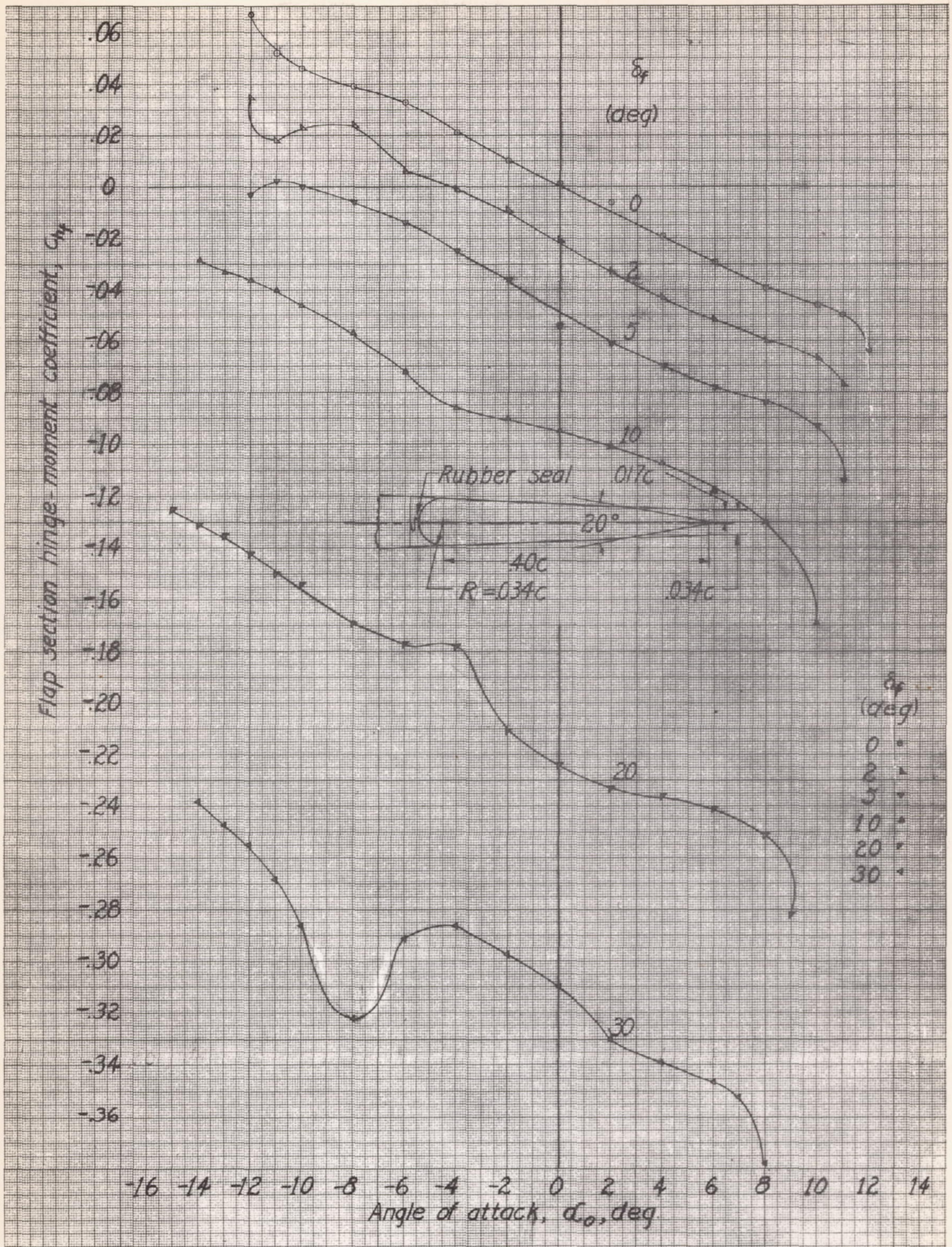

Figure 11.- Concluded.

L-666

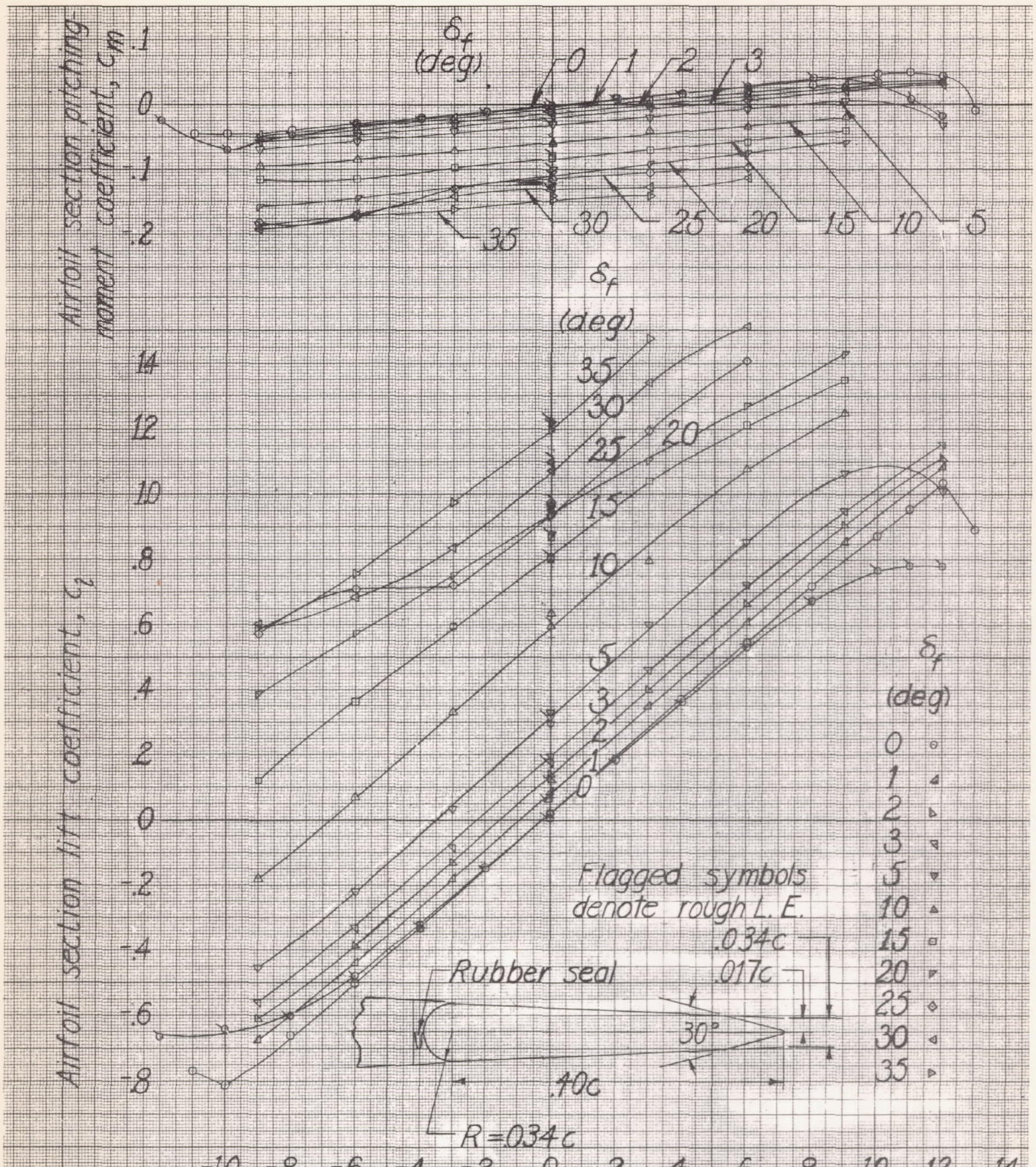

Figure 12.- Aerodynamic section characteristics of an NACA 0009 airfoil having 0.40c flap with 30° beveled trailing edge. Sealed gap; q = 15 pounds per square foot.

L-666

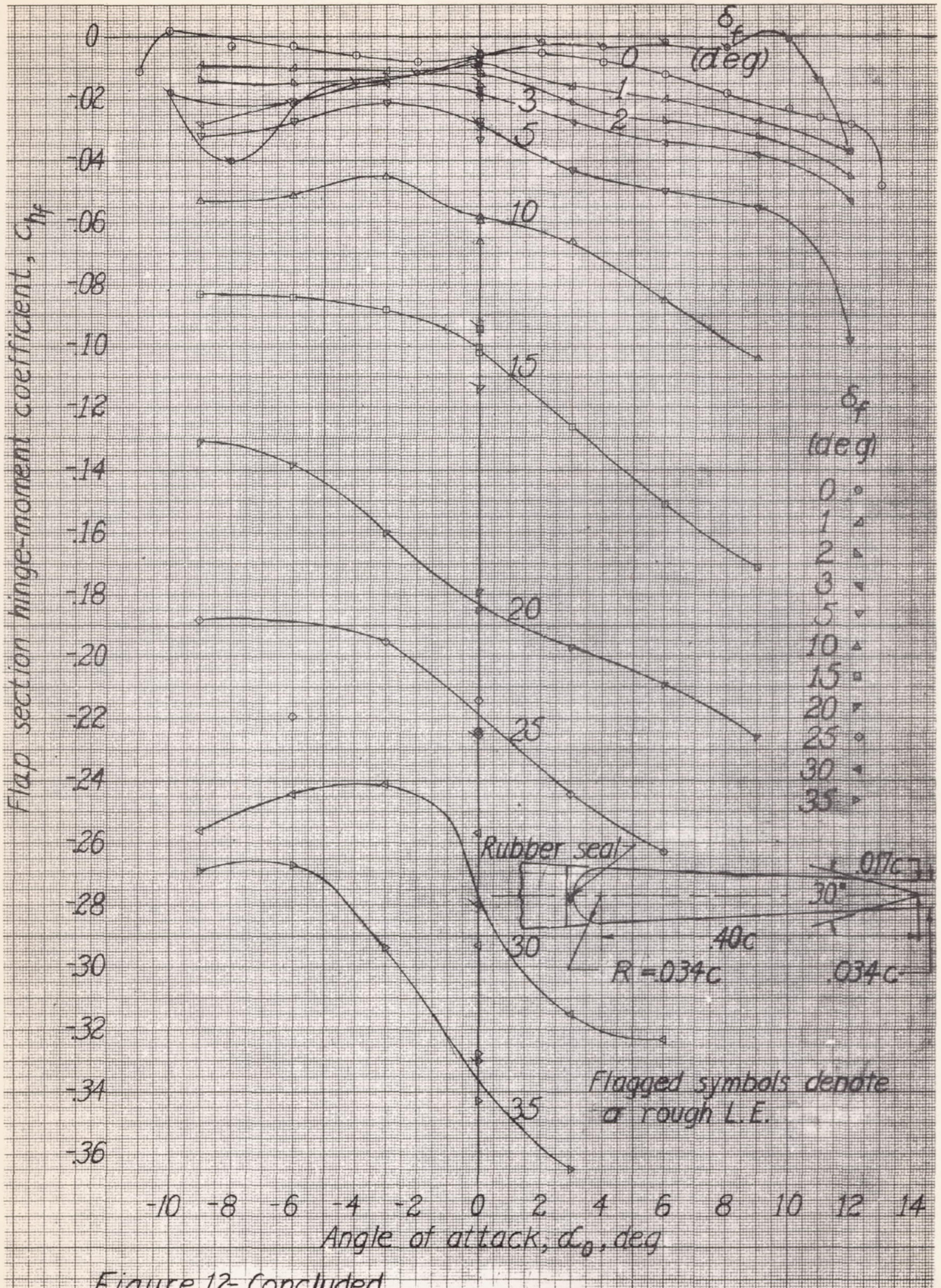

Figure 12- Concluded.

L-666

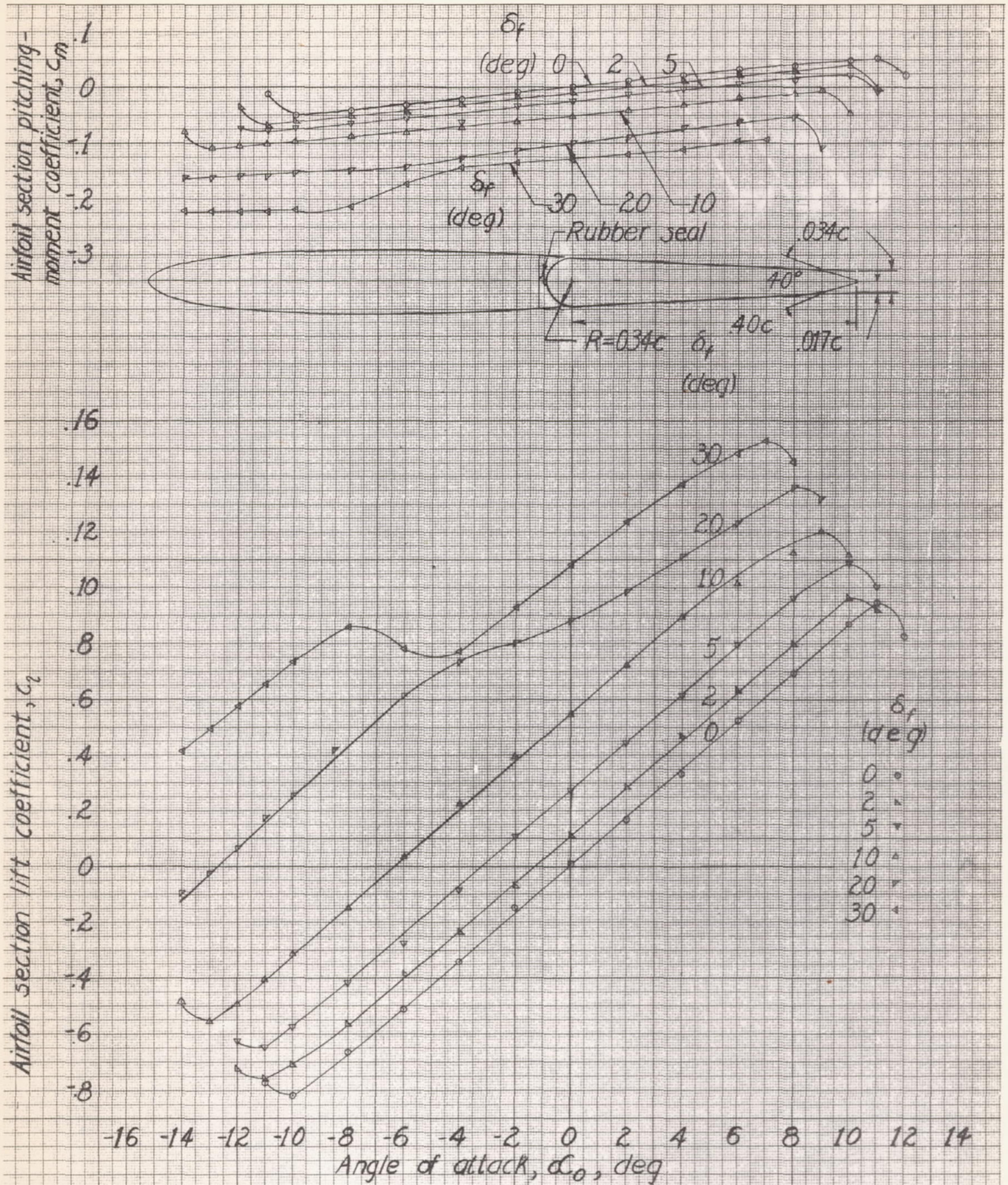

Figure 13.- Aerodynamic section characteristics of an NACA 0009 airfoil having 0.40c flap with 40° beveled trailing edge. Sealed gap; q = 11.25 pounds per square foot.

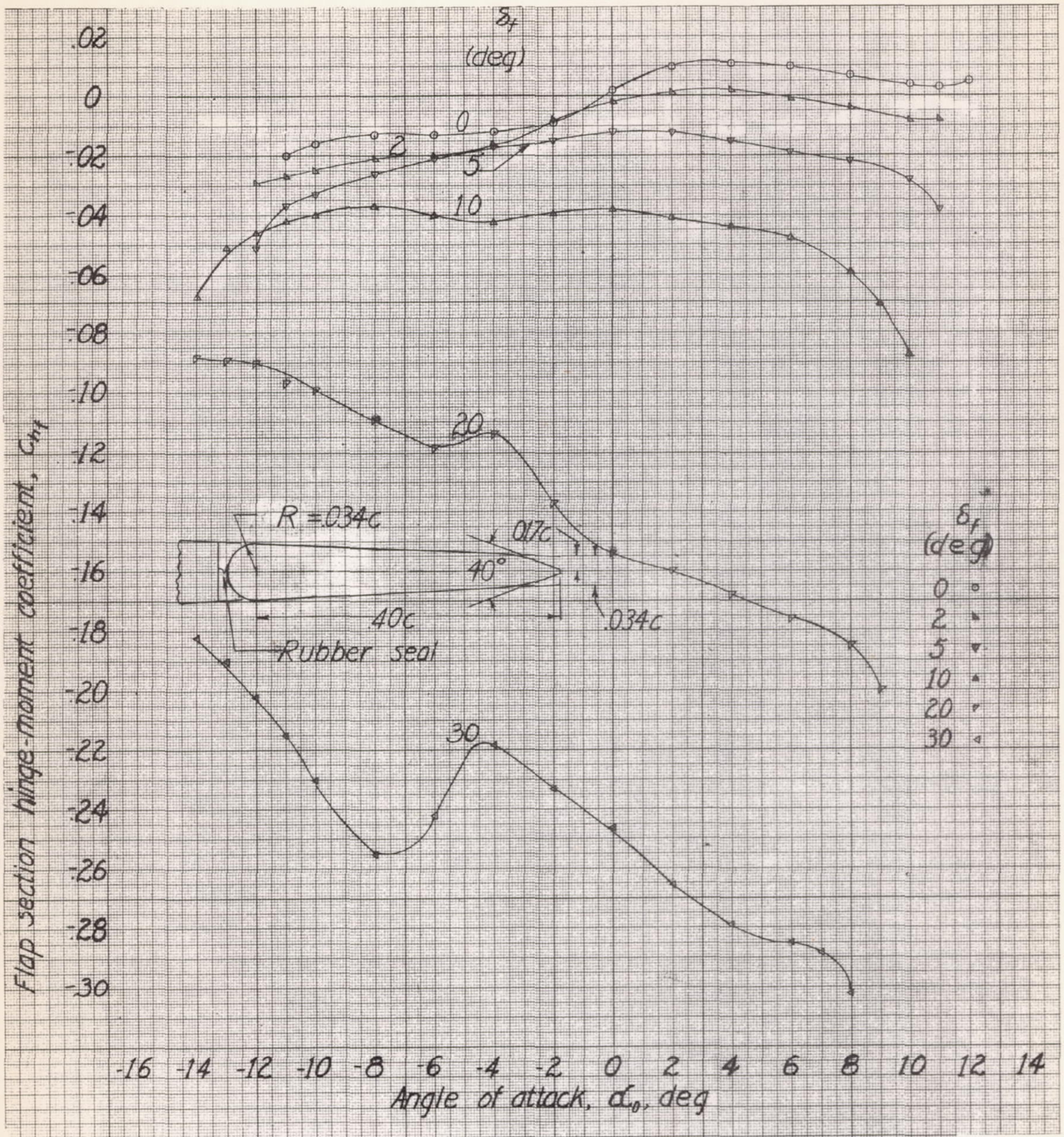

Figure 13.- Concluded.

L-666

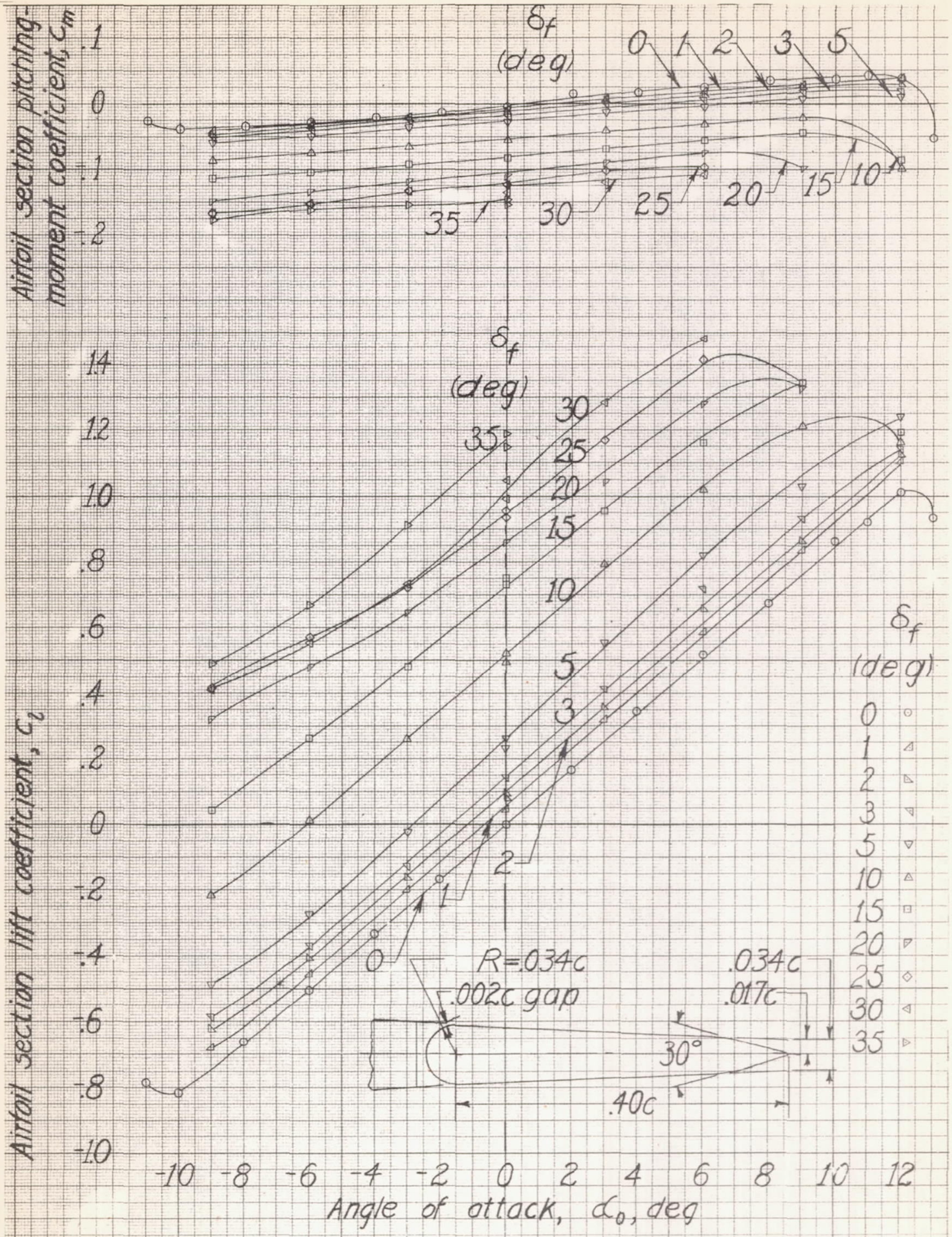

Figure 14.-Aerodynamic section characteristics of NACA 0009 airfoil having 0.40c flap with 30° beveled trailing edge. 0.002c gap; q=15 pounds per square foot.

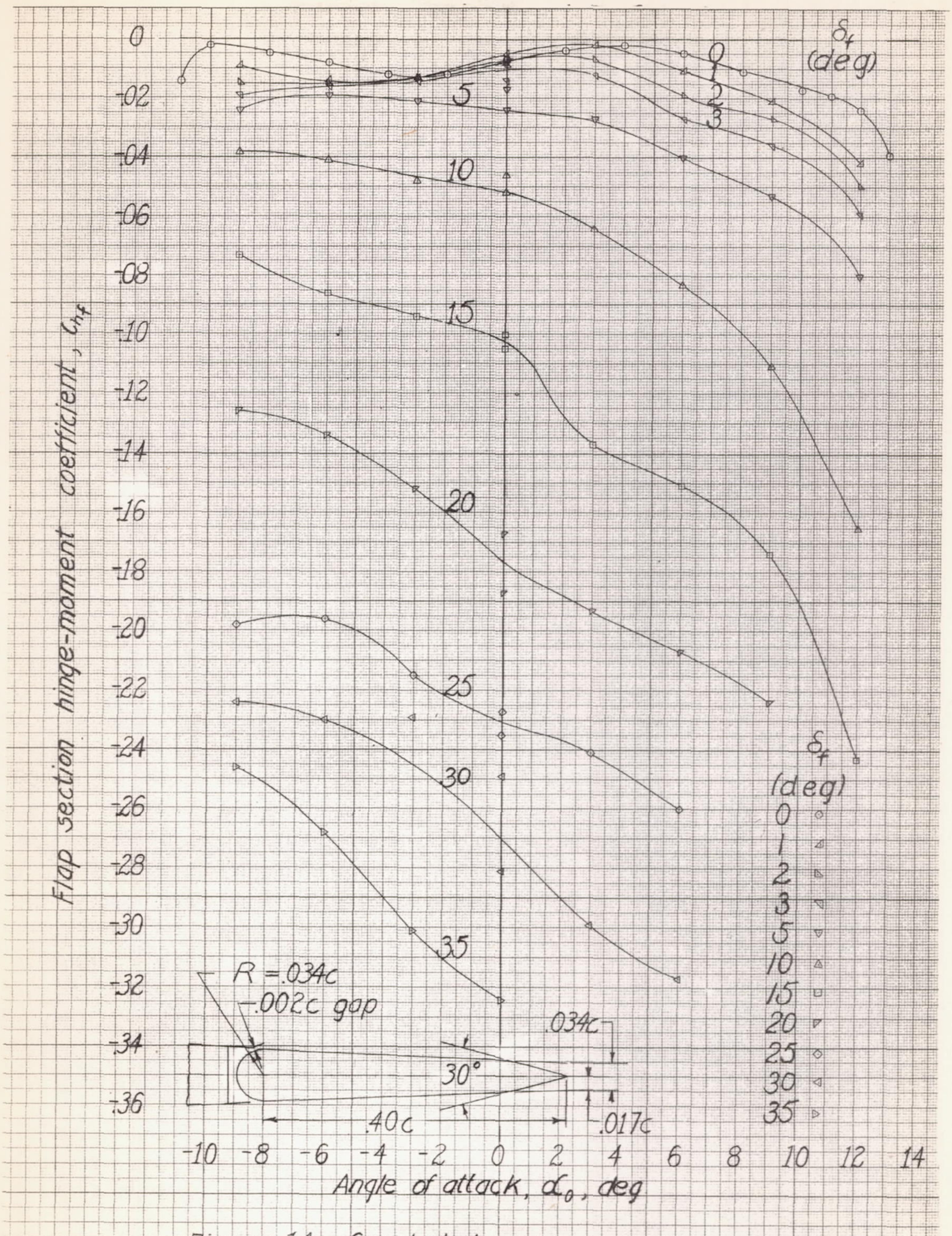

Figure 14.- Concluded.

L-666

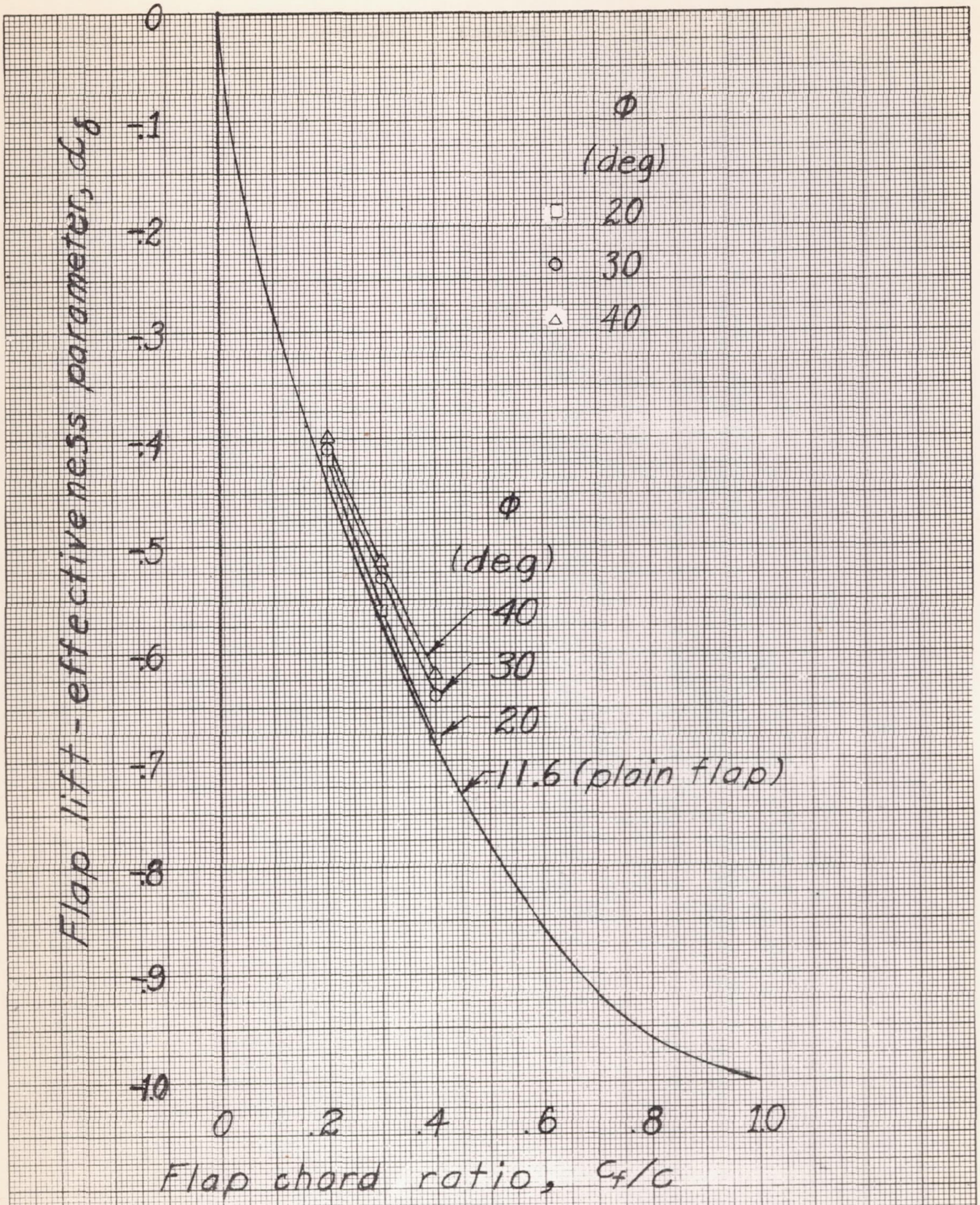

Figure 15.-Variation of flap lift-effectiveness parameter with flap chord ratio. Sealed gap. Plain-flap curve from figure 141 reference 3.

L-666

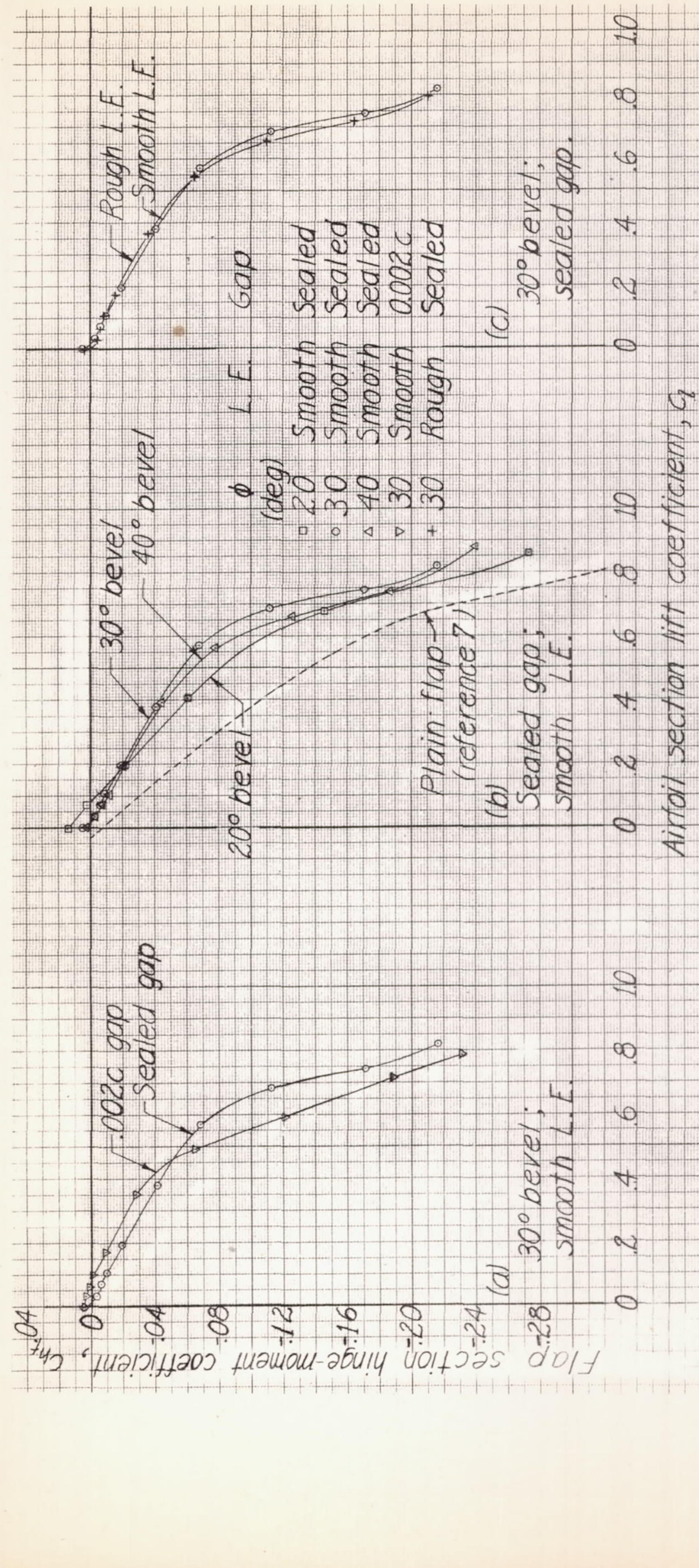

Figure 16.-Variation of flap section hinge-moment coefficient with airfoil section lift coefficient for a 0.20c flap from $\delta_f = 0°$ to $\delta_f = 30°$. $\alpha_o = 0°$.

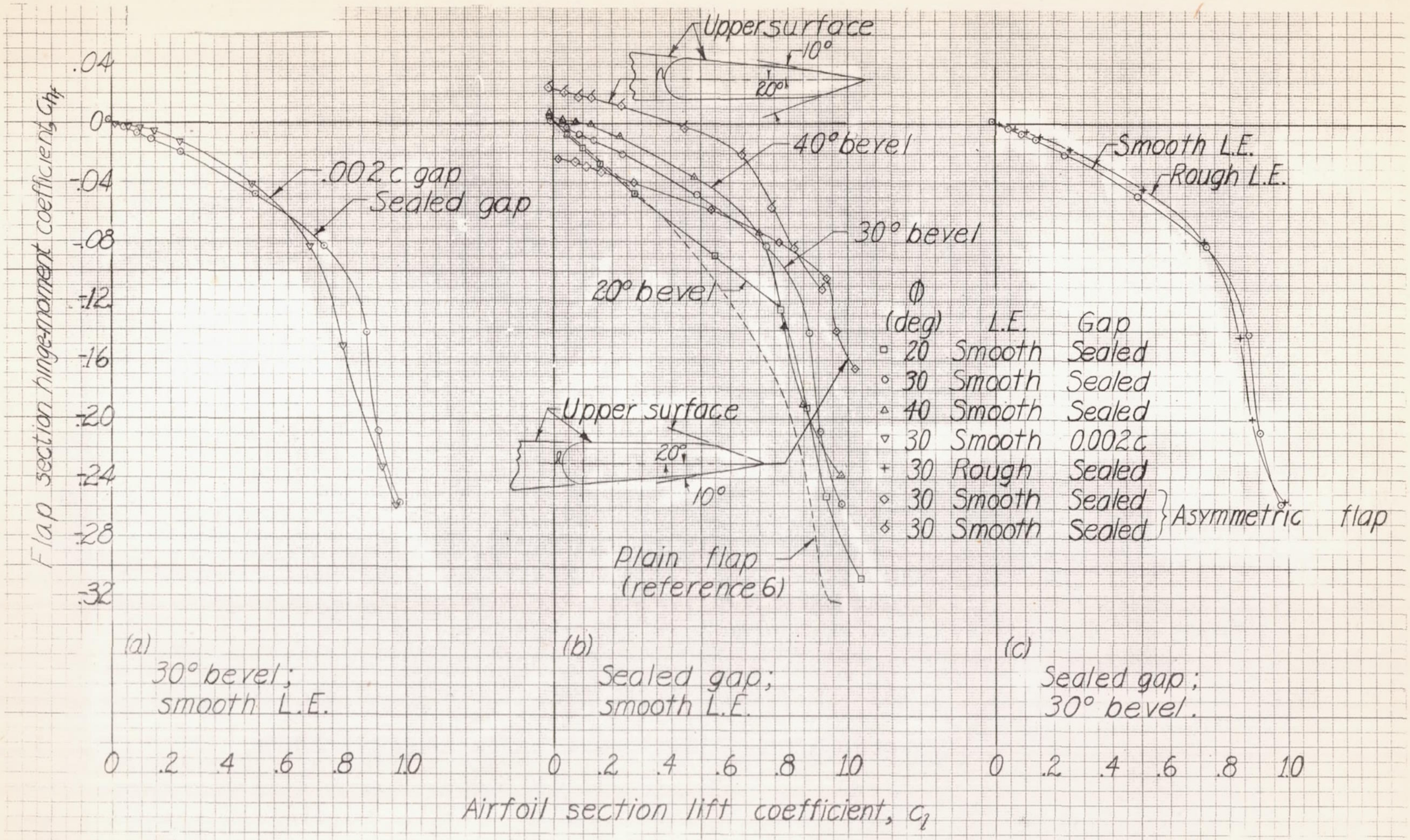

Figure 17.- Variation of flap section hinge-moment coefficient with airfoil section lift coefficient for a 0.30c flap from $\delta_f = 0°$ to $\delta_f = 30°$. $\alpha_0 = 0°$.

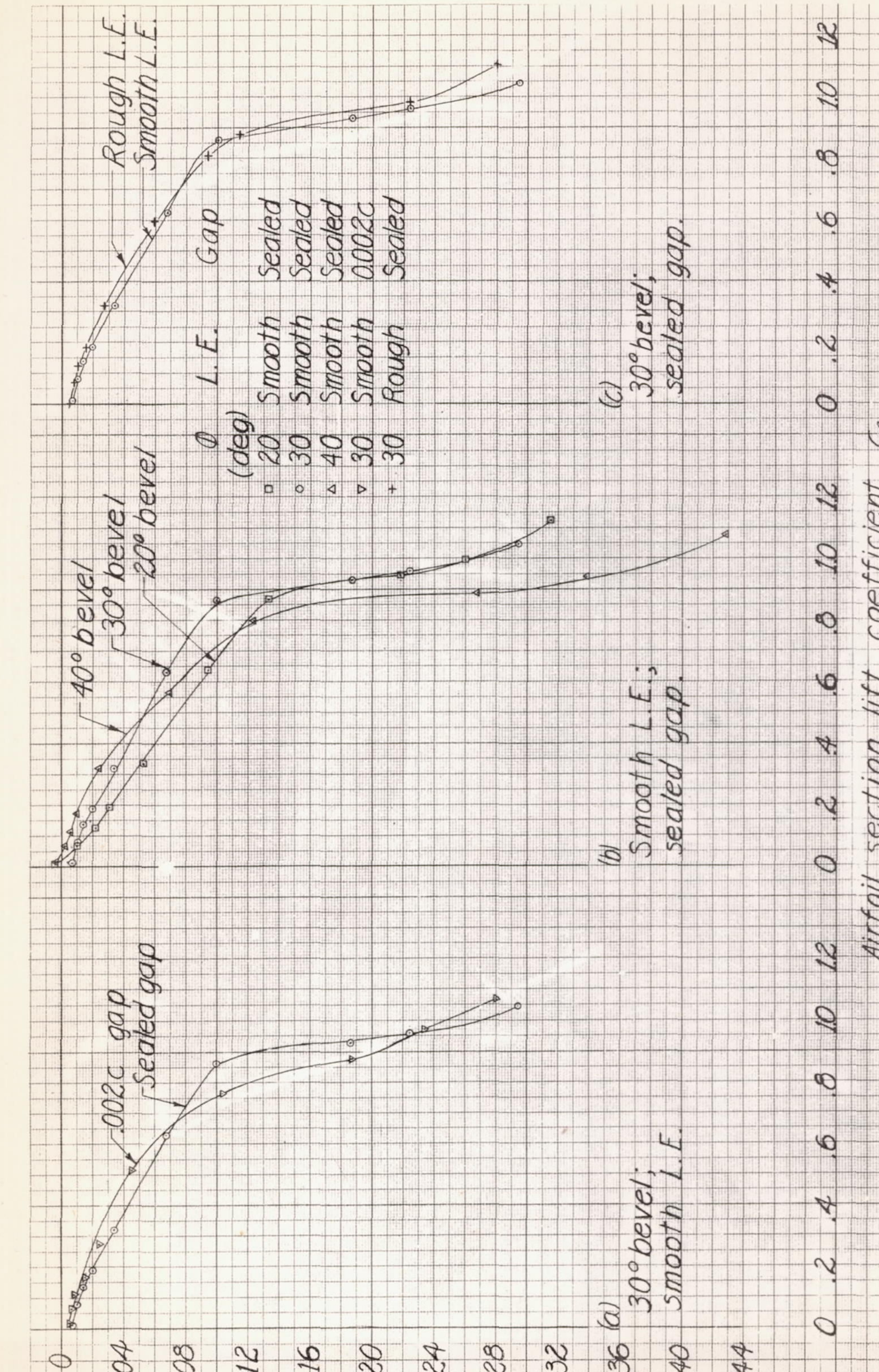

Figure 18-Variation of flap section hinge-moment coefficient with airfoil section lift coefficient for a 0.40c flap from $\delta_f = 0°$ to $\delta_f = 30°$. $\alpha_0 = 0°$.

L-666

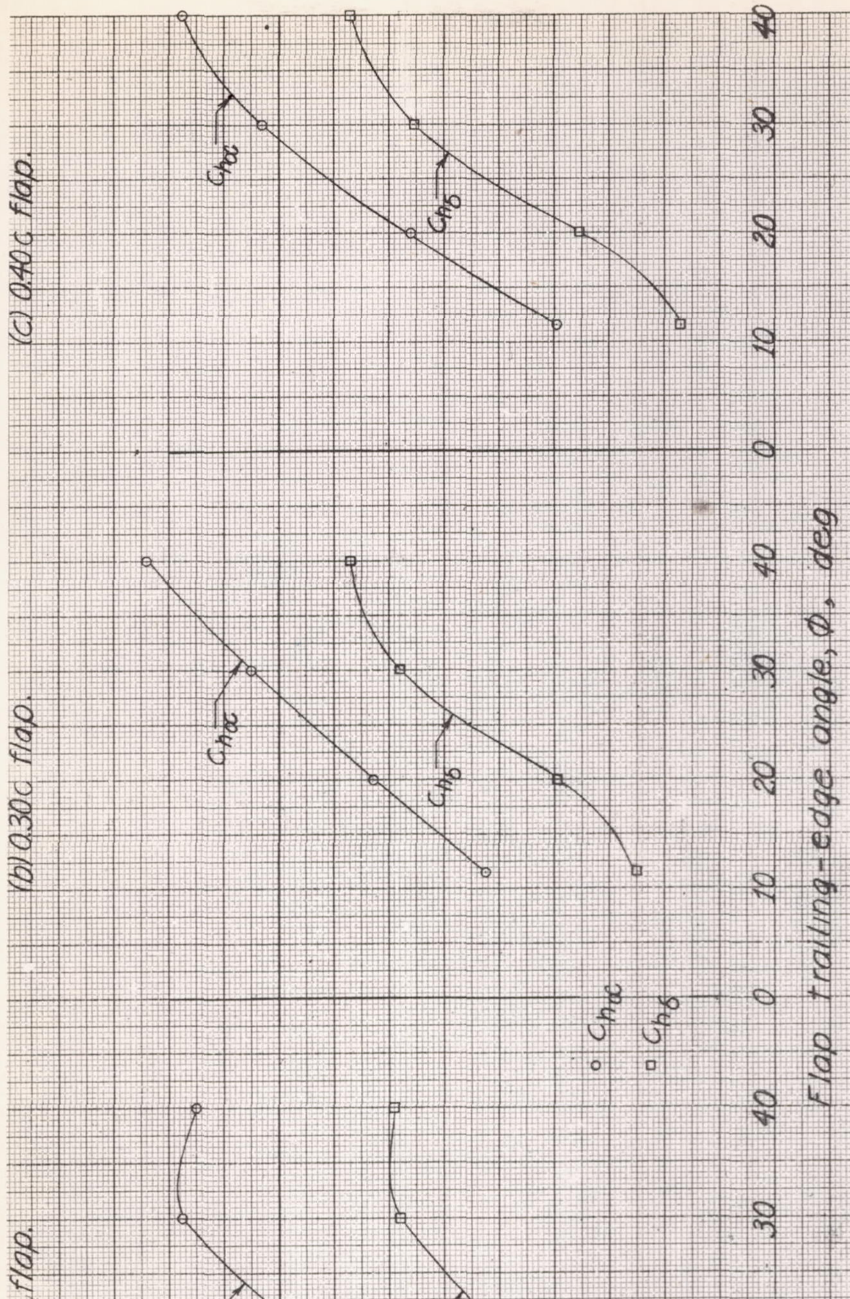

Figure 19.- Variation of flap section hinge-moment parameters with flap trailing-edge angle. Sealed gap. Values at ϕ = 11.6° from reference 3.

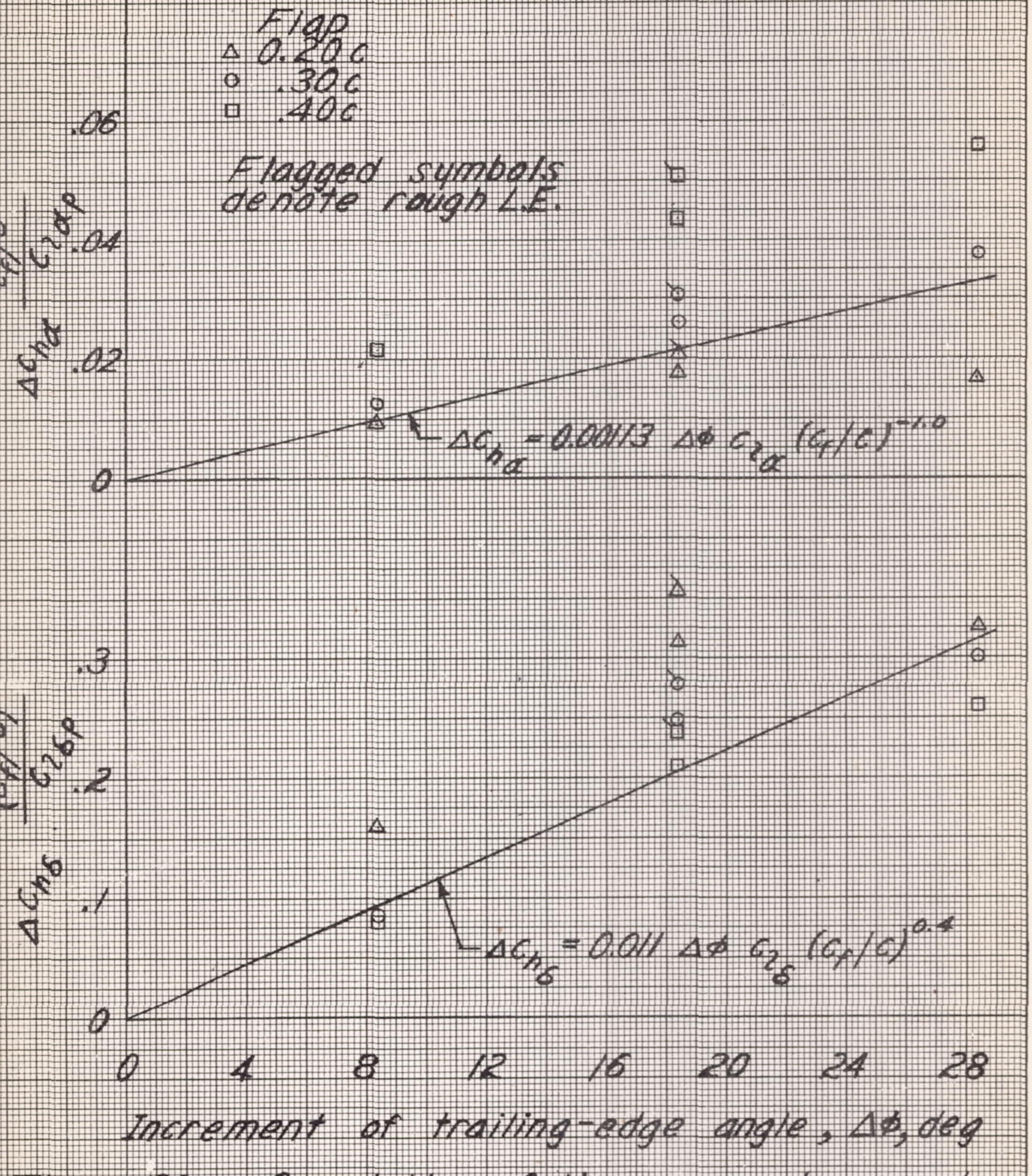

Figure 20.- Correlation of hinge-moment parameters for beveled-trailing-edge flaps on basis of trailing-edge angle for NACA 0009 airfoil of present investigation. Sealed gap. Method used from figure 150, reference 6, which is adapted from reference 4.

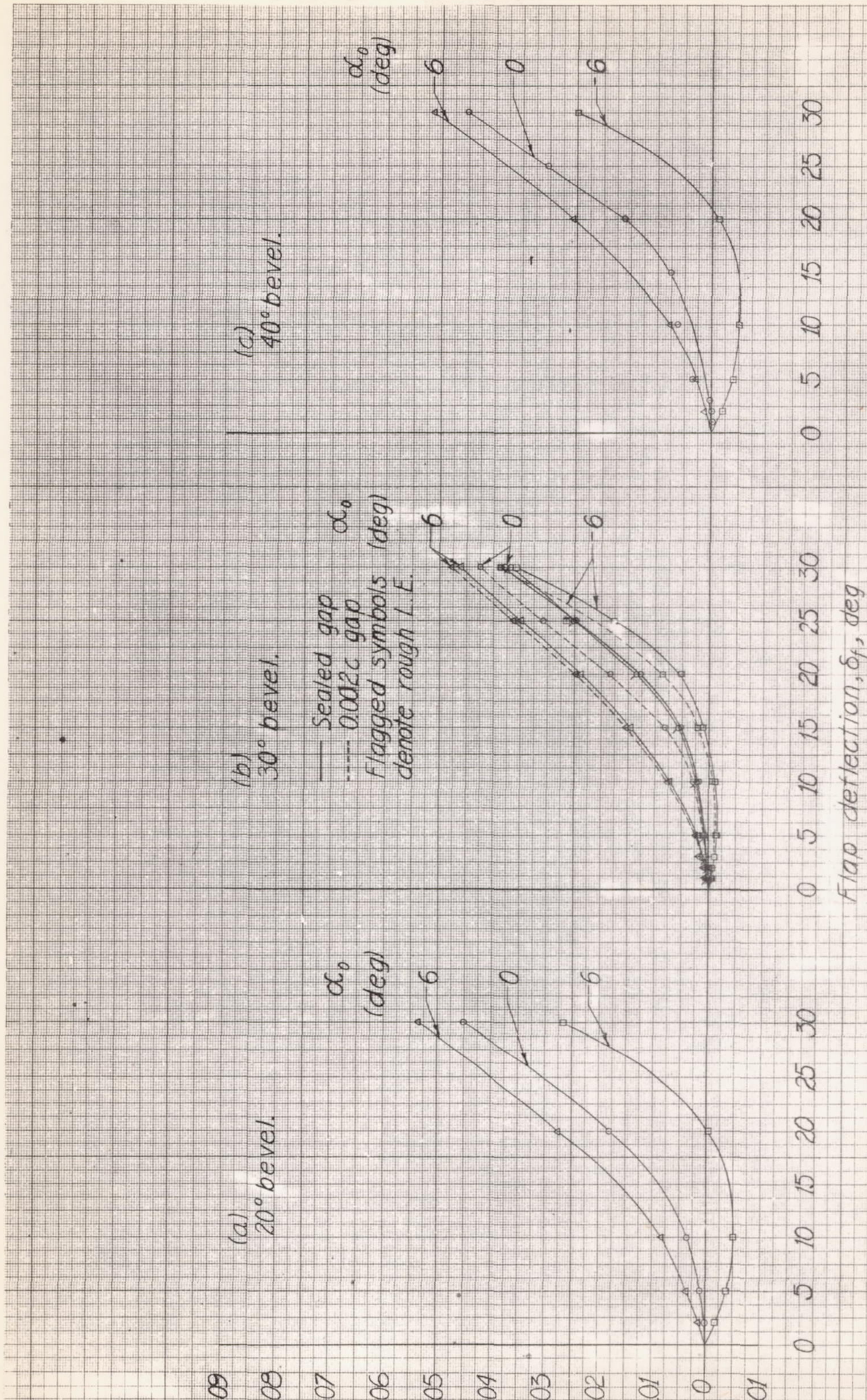

Figure 21.- Increment of airfoil section profile-drag coefficient caused by deflection of a 0.20c flap with three beveled trailing edges. Smooth L.E. except as indicated.

L-666

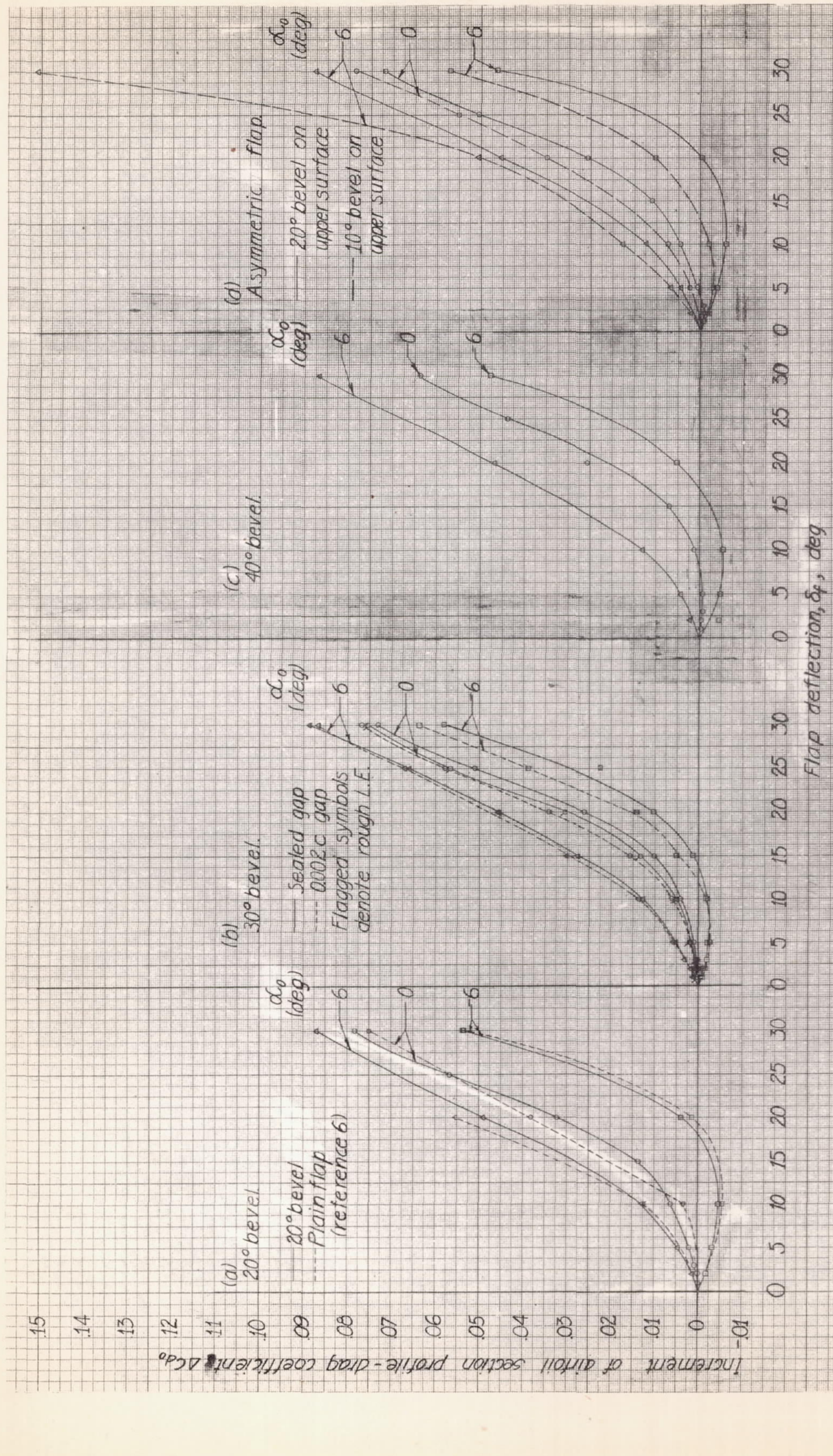

Figure 22.- Increment of airfoil section profile-drag coefficient caused by deflection of a 0.30c flap with four beveled trailing edges. Smooth L.E. except as indicated.

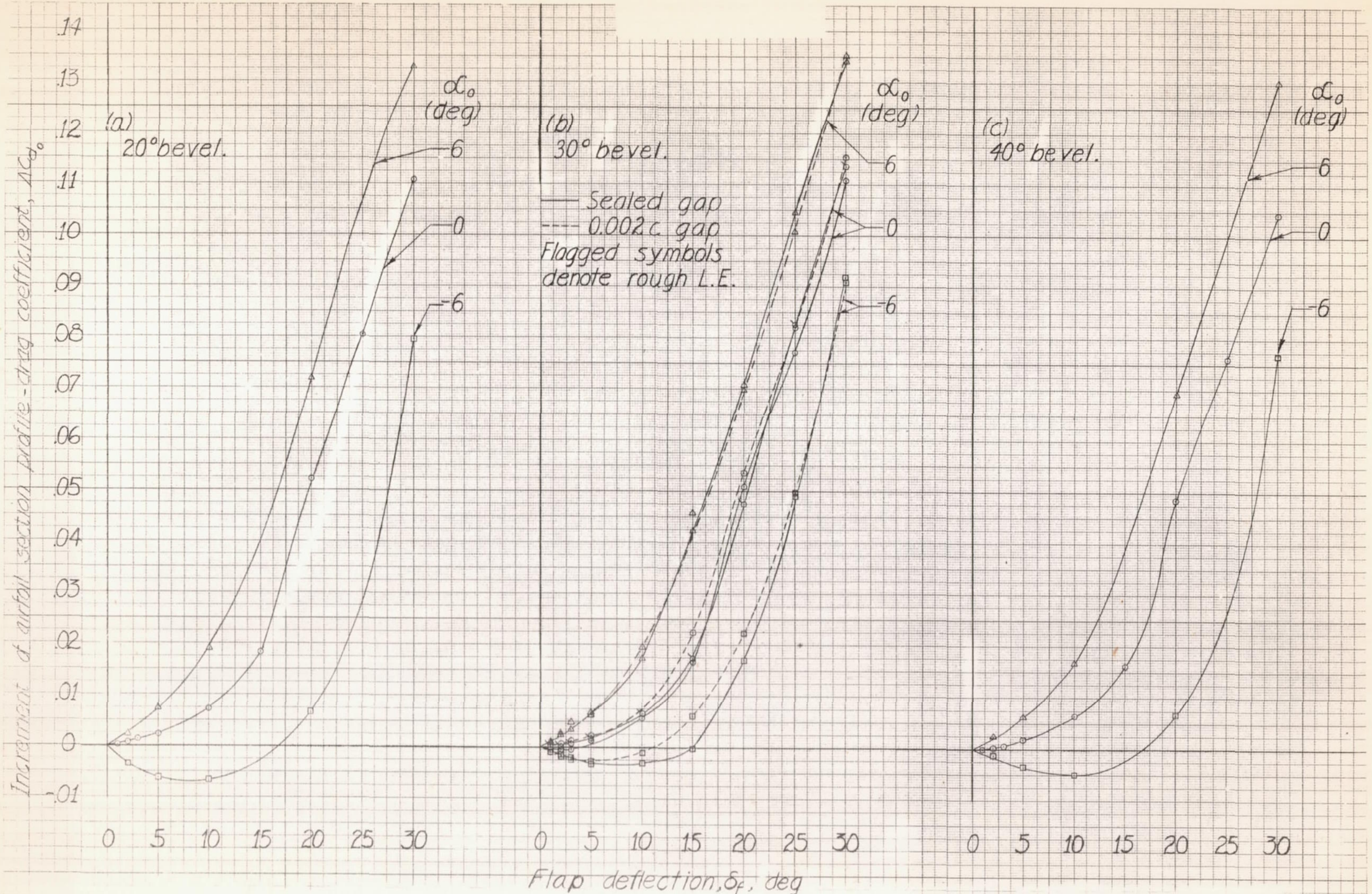

Figure 23.- Increment of airfoil section profile-drag coefficient caused by deflection of a 0.40c flap with three beveled trailing edges. Smooth L.E. except as indicated.

L-666

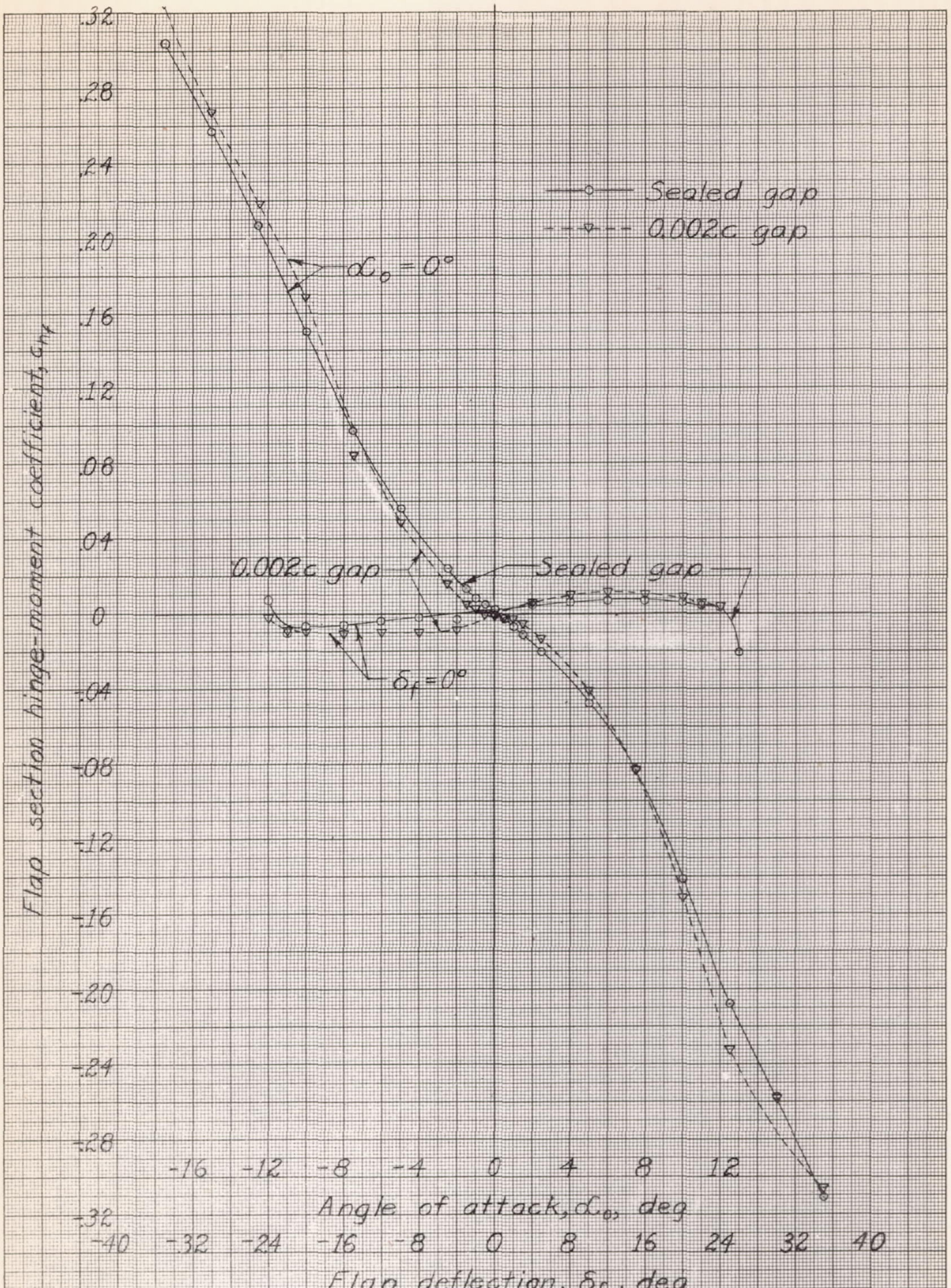

Figure 24.- Effect of a 0.002c gap on the hinge-moment characteristics of a 0.30c flap with a 30° beveled trailing edge and smooth leading edge.

L-666

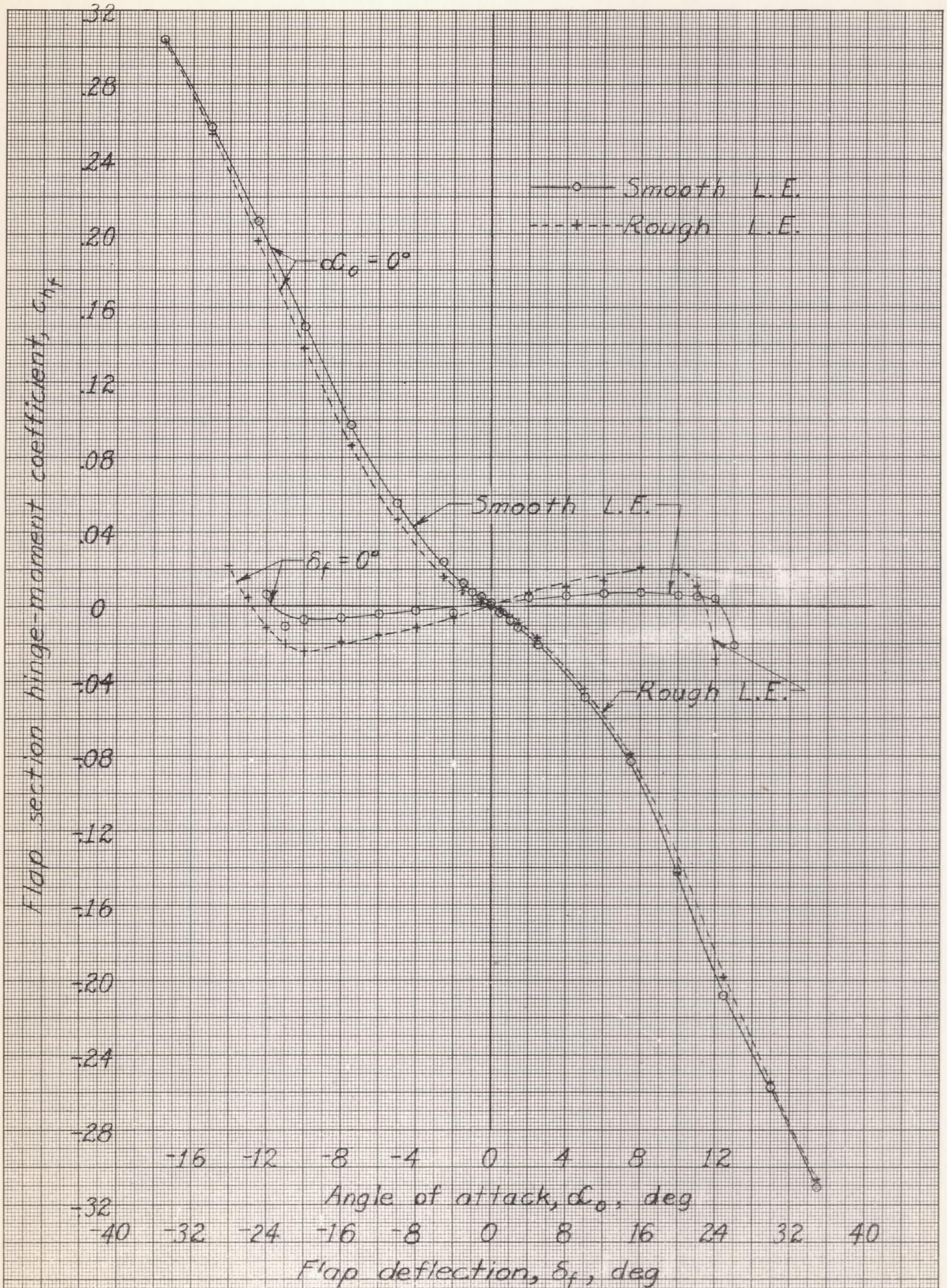

Figure 25.-Effect of a rough leading edge on the hinge moment characteristics of a 0.30c flap with a 30° beveled trailing edge and sealed gap.